UNIVERSITI PUTRA MALAYSIA

DEGRADATION PHENOMENA IN PRASEODYMIUM OXIDE-BASED ZINC OXIDE VARISTOR CERAMICS DERIVED THROUGH MODIFIED CITRATE TECHNIQUE

WAN RAFIZAH BINTI WAN ABDULLAH @ WAN ABD. RAHMAN

ITMA 2014 1

DEGRADATION PHENOMENA IN PRASEODYMIUM OXIDE-BASED ZINC OXIDE VARISTOR CERAMICS DERIVED THROUGH MODIFIED CITRATE TECHNIQUE

By

WAN RAFIZAH BINTI WAN ABDULLAH @ WAN ABD. RAHMAN

Thesis Submitted to the School of Graduate Studies, Universiti Putra Malaysia, in Fulfilment of the Requirements for the Degree of Doctor of Philosophy

August 2014

© COPYRIGHT UPM

COPYRIGHT

All material contained within the thesis, including without limitation text, logos, icons, photographs and all other artworks, is copyright material of Universiti Putra Malaysia unless otherwise stated. Use may be made of any material contained within the thesis for non-commercial purposes from the copyright holder. Commercial use of material may only be made with the express, prior, written permission of Universiti Putra Malaysia.

Copyright © Universiti Putra Malaysia

© COPYRIGHT UPM

Abstract of thesis presented to the Senate of Universiti Putra
Malaysia in fulfilment of the requirement for the degree of Doctor of Philosophy

DEGRADATION PHENOMENA IN PRASEODYMIUM OXIDE-BASED ZINC OXIDE VARISTOR CERAMICS DERIVED THROUGH MODIFIED CITRATE TECHNIQUE

By

WAN RAFIZAH BINTI WAN ABDULLAH @ WAN ABD. RAHMAN

August 2014

Chairman: Azmi Bin Zakaria, PhD
Faculty: Institute of Advanced Technology

Current trend shows that Pr_6O_{11} based ZnO ceramics are actively researched to overcome drawbacks in Bi_2O_3 based varistor materials. However, very little attention has been paid to evaluate the stability of these materials against DC degradation which causes reduction of device lifetime and poses safety risks to users. DC degradation characteristics of four series of Pr_6O_{11} type ceramics prepared through modified citrate gelation technique and solid state sintering are therefore investigated. The series are System 1 (ZnO + Pr_6O_{11}), System 2 (ZnO + Pr_6O_{11} + Co_3O_4), System 3 (ZnO + Pr_6O_{11} + MnO_2) and System 4 (ZnO + Pr_6O_{11} + Cr_2O_3). The objectives of the present study were to determine the microstructure and nonlinear properties as a function of dopant contents and sintering conditions, to evaluate the degradation effects due to simultaneous DC electrical field and high temperature stresses on nonlinear properties of respective varistor system and to investigate the influence of deep levels on varistor degradation by using deep level transient spectroscopy (DLTS) technique. The ceramics were characterized in terms of microstructure profiles, electrical field-current density characteristics, DC degradation behaviour and deep level characteristics.

Several important findings of the study are highlighted. $PrCrO_3$ spinel has been developed in varistor ceramics doped with 0.8 mol% Pr_6O_{11} and 1.0 mol% Cr_2O_3. To certain extent, Pr_6O_{11} and Cr_2O_3 suppress grain growth. The average grain size, d and average relative density, ρ_{rel} decreased with increasing Pr_6O_{11} and Cr_2O_3 contents. Co_3O_4 and MnO_2 promoted grain growth and densification. Therefore, the d and ρ_{rel} values increased with their increasing contents. Electrically, Pr_6O_{11} served as grain boundary activator whereas Co_3O_4, MnO_2 and Cr_2O_3 further enhanced the nonlinearity.

© COPYRIGHT UPM

The nonlinear coefficient, α and breakdown field, E_b values increased and the leakage current density, J_L value decreased up to certain extent of dopant contents. In the temperature range of 1200 to 1275 ^oC, most systems demonstrated that d and ρ_{rel} values improved with increasing sintering temperature. Similar trend was observed when the sintering time was varied between 1 to 7 hours. Nonlinear properties were improved with increasing sintering temperature and time until an optimum point was reached. Extreme sintering temperature and extended sintering time deteriorate nonlinear characteristics.

Ceramics with the highest ρ_{rel} value (97.88 $\pm$ 0.28 %) were obtained from System 1. The ceramics were doped with only 0.2 mol% Pr_6O_{11} and sintered at 1225 ^oC for 1 hour. Ceramics with the largest d value (18.62 $\pm$ 4.16 μm) were identified in System 2 which contained 0.8 mol% Pr_6O_{11} and 0.4 mol% Co_3O_4. They were sintered at 1250 ^oC for 3 hours. The most pronounced nonlinearity was observed in ceramics of System 4 which were doped with 0.8 mol% Pr_6O_{11} and 0.6 mol% Cr_2O_3. The corresponding ceramics have been sintered at 1200 ^oC for 1 hour and demonstrated the α value of 6.04 $\pm$ 0.02, the E_b value of 127.05 $\pm$ 0.38 V/mm and the J_L value of 327 $\pm$ 1 μA/cm^2.

All systems degraded under three stages of stress conditions. At each stage, DC electrical field of 85% from the breakdown field was applied for 18 hours whereas the temperature was increased from 30 to 60 and 125 ^oC in the subsequent stages. The signs of degradation included a decrease in the α value, the shifting of E_b value to a lower field and a rise in the J_L value. Ceramic of System 4 demonstrated the best tolerance to DC degradation compared to the rest by exhibiting $\%\Delta E_b$ value of -9.86%, the $\%\Delta\alpha$ of -4.37% and the $\%\Delta J_L$ of +13.73%. Comparatively, some Pr_6O_{11} based ZnO varistor ceramics obtained in this study exhibited better stability against DC electrical field and temperature stress than the more complex Bi_2O_3 based ZnO ceramics prepared through similar citrate gel method. As previously reported, chemically derived Bi_2O_3 based ZnO ceramics that have been doped with more additives such as Sb_2O_3, MnO, Al_2O_3, Co_2O_3, NiO, Cr_2O_3 demonstrated the $\%\Delta E_b$ value of 1.5%, $\%\Delta\alpha$ of up to -37.5%, and the $\%\Delta J_L$ of +323% when subjected to comparable three stages of DC electrical field and high temperature stresses.

DLTS technique confirmed the presence of four electron traps in Pr_6O_{11} based ceramics. The bulk trap, L1 and L2 respectively located (0.09 - 0.15 eV) and (0.29 - 0.39 eV) below the conduction band edge. They were associated to intrinsic donor defects (V_o and Zn_i) or the complex with extrinsic donor defects (Mn or Co). The interface states, L3 and/or L4 located between 0.45 to 0.91 eV below the conduction band edge and they were associated to defect clusters of zinc vacancy, V_{Zn}, adsorbed or chemisorbed oxygen and impurities (Pr, Mn or Co). In degraded state, the densities of L1 and L3 traps for System 1 and 4 have reduced due to annihilation of defects and desorption of oxygen from grain boundary during stress application. The L3 trap in System 4 shifted to a higher energy because of new defect clusters formation. In System 2 and 3, the density

of L1 trap increased after degradation test due to an increase in intrinsic defects such as V_o and Zn_i and extrinsic donor defects in depletion regions. It was accompanied by an increase in density of L3 (System 2) and L4 (System 3) traps which was associated to ionization of mid-gap states induced by Co or Mn.

In conclusion, degradation of Pr_6O_{11} based ZnO varistor ceramics which were doped with transition metal oxide (Co_3O_4, MnO_2 or Cr_2O_3) and derived from modified citrate gel technique due to prolonged DC electrical field and high temperature stresses was a direct effect to Double Schottky Barrier deformation. The degradation mechanisms were governed by electromigration and oxygen desorption processes which induced by chemical and electronic changes centering at grain boundary interface.

© COPYRIGHT UPM

Abstrak tesis yang dikemukakan kepada Senat Universiti Putra Malaysia
sebagai memenuhi keperluan untuk ijazah Doktor Falsafah

FENOMENA KEMEROSOTAN DALAM SERAMIK VARISTOR ZINK OKSIDA BERASASKAN PRASEODIMIUM OKSIDA DITERBITKAN MELALUI TEKNIK SITRAT TERUBAHSUAI

Oleh

WAN RAFIZAH BINTI WAN ABDULLAH @ WAN ABD. RAHMAN

Ogos 2014

Pengerusi: Azmi Bin Zakaria, PhD
Fakulti: Institut Teknologi Maju

Kecenderungan terkini menunjukkan bahawa seramik ZnO berasaskan Pr_6O_{11} dikaji secara aktif untuk mengatasi kekurangan bahan varistor berasaskan Bi_2O_3. Namun, kurang perhatian diberikan untuk menilai kestabilan bahan ini terhadap kemerosotan AT yang mengakibatkan penurunan jangka hayat peranti dan mendedahkan risiko keselamatan terhadap pengguna. Ciri-ciri kemerosotan AT bagi empat siri seramik Pr_6O_{11} yang disediakan melalui teknik pengegelan sitrat terubahsuai dan pensinteran keadaan pepejal dengan itu disiasat. Siri-siri berkenaan adalah Sistem 1 (ZnO + Pr_6O_{11}), Sistem 2 (ZnO + Pr_6O_{11} + Co_3O_4), Sistem 3 (ZnO + Pr_6O_{11} + MnO_2) dan Sisyem 4 (ZnO + Pr_6O_{11} + Cr_2O_3). Objektif kajian ini adalah untuk menentukan sifat-sifat mikrostruktur dan ketaklinearan sebagai satu fungsi kandungan pendopan dan keadaan pensinteran, untuk menilai kesan-kesan kemerosotan oleh kerana tekanan medan elektrik AT dan suhu tinggi serentak terhadap sifat-sifat ketaklinearan bagi setiap sistem dan untuk menyiasat pengaruh aras-aras dalam terhadap kemerosotan varistor menggunakan teknik spektroskopi fana aras dalam (DLTS). Seramik-seramik dicirikan mengikut profil mikrostruktur, ciri-ciri medan elektrik - ketumpatan arus, kelakuan kemerosotan AT dan ciri-ciri aras dalam.

Beberapa penemuan penting daripada kajian ini ditegaskan. Spinel $PrCrO_3$ telah pun dibangunkan dalam seramik varistor terdop dengan 0.8 mol% Pr_6O_{11} and 1.0 mol% Cr_2O_3. Sehingga ke takat tertentu, Pr_6O_{11} dan Cr_2O_3 menahan pertumbuhan butir. Saiz butir purata, d dan ketumpatan relatif purata, ρ_{rel} menurun dengan peningkatan kandungan Pr_6O_{11} dan Cr_2O_3. Co_3O_4 dan MnO_2 menggalakkan pertumbuhan butir dan penumpatan. Maka, nilai d dan ρ_{rel} meningkat dengan peningkatan kandungannya.

© COPYRIGHT UPM

Secara elektrik, Pr_6O_{11} berfungsi sebagai pengaktif sempadan butir manakala Co_3O_4, MnO_2 and Cr_2O_3 selanjutnya mempertingkatkan ketaklinearan. Nilai pekali ketaklinearan, α dan medan runtuh, E_b meningkat dan ketumpatan arus bocor, J_L menurun sehingga ke suatu takat kandungan pendopan. Di dalam julat suhu 1200 hingga 1275 ^oC, kebanyakan sistem menunjukkan bahawa nilai d dan ρ_{rel} bertambahbaik dengan peningkatan suhu pensinteran. Kecenderungan yang sama diperhatikan apabila masa pensinteran diubah di antara 1 ke 7 jam. Sifat-sifat ketaklinearan bertambah baik dengan peningkatan suhu dan masa pensinteran sehingga suatu titik optimum dicapai. Suhu pensinteran ekstrem dan masa pensinteran lanjutan memusnahkan ciri-ciri ketaklinearan.

Seramik dengan nilai ρ_{rel} tertinggi (97.88 $\pm$ 0.28 %) diperolehi daripada Sistem 1. Seramik tersebut didop dengan hanya 0.2 mol% Pr_6O_{11} dan disinter pada 1225 ^oC selama 1 jam. Seramik dengan nilai d terbesar (18.62 $\pm$ 4.16 μm) telah dikenalpasti dalam Sistem 2 yang mengandungi 0.8 mol% Pr_6O_{11} dan 0.4 mol% Co_3O_4. Ia telah disinter pada 1250 ^oC selama 3 jam. Ketaklinearan paling ketara telah diperhatikan dalam seramik Sistem 4 yang didop dengan 0.8 mol% Pr_6O_{11} dan 0.6 mol% Cr_2O_3. Seramik berkenaan telah pun disinter pada 1200 ^oC selama 1 jam. Seramik yang terhasil menunjukkan nilai α sebanyak 6.04 $\pm$ 0.02, nilai E_b sebanyak 127.05 $\pm$ 0.38 V/mm dan nilai J_L sebanyak 327 $\pm$ 1 μA/cm^2.

Semua sistem merosot di bawah keadaan tiga peringkat tekanan. Pada setiap peringkat, medan elektrik AT setinggi 85% daripada medan runtuh telah dikenakan selama 18 jam manakala suhu ditingkatkan dari 30 ke 60 dan 125 ^oC pada peringkat berikutnya. Tanda-tanda kemerosotan termasuk penurunan dalam nilai α, anjakan nilai E_b ke medan lebih rendah dan kenaikan dalam nilai J_L. Seramik bagi Sistem 4 menunjukkan ketahanan terbaik terhadap kemerosotan AT berbanding yang lain dengan mempamerkan $\%\Delta E_b$ sebanyak -9.86%, nilai $\%\Delta\alpha$ sebanyak -4.37% dan nilai $\%\Delta J_L$ sebanyak +13.73%. Secara perbandingannya, sebahagian seramik varistor ZnO berasaskan Pr_6O_{11} yang diperoleh dalam kajian ini menunjukkan kestabilan lebih baik terhadap tekanan medan elektrik AT dan suhu daripada seramik ZnO berasaskan Bi_2O_3 lebih kompleks yang disediakan melalui kaedah pengejelan sitrat yang serupa. Seperti yang dilaporkan sebelum ini, seramik ZnO berasaskan Bi_2O_3 terbitan secara kimia yang terdop dengan lebih banyak tambahan seperti Sb_2O_3, MnO, Al_2O_3, Co_2O_3, NiO, Cr_2O_3 menunjukkan nilai $\%\Delta E_b$ sebanyak 1.5%, $\%\Delta\alpha$ sehingga -37.5%, dan $\%\Delta J_L$ sebanyak +323% apabila dikenakan tiga peringkat tekanan setara medan elektrik AT dan suhu tinggi.

Teknik DLTS mengesahkan kehadiran empat perangkap elektron di dalam seramik berasaskan Pr_6O_{11}. Perangkap pukal, L1 dan L2 masing-masing terletak (0.09 - 0.15 eV) dan (0.29 - 0.39 eV) di bawah pinggir jalur konduksi. Ia dikaitkan dengan kecacatan penderma dalam (V_o dan Zn_i) atau kompleks dengan kecacatan penderma luar (Mn atau Co). Perangkap antaramuka, L3 dan/atau L4 terletak di antara 0.45 to 0.91 eV di bawah pinggir jalur konduksi dan ia dikaitkan dengan kelompok kecacatan bagi kekosongan

zink, V_{Zn}, oksigen terjerap atau terjerap kimia dan bendasing (Pr, Mn atau Co). Dalam keadaan merosot, ketumpatan perangkap L1 dan L3 dalam Sistem 1 dan 4 menurun oleh kerana pemusnahan kecacatan dan penyahjerapan oksigen daripada sempadan butir semasa penggunaan tekanan. Perangkap L3 dalam Sistem 4 beranjak ke tenaga lebih tinggi kerana pembentukan kelompok kecacatan yang baru. Di dalam Sistem 2 dan 3, ketumpatan perangkap L1 meningkat selepas ujian kemerosotan disebabkan oleh peningkatan dalam kecacatan dalam seperti V_o dan Zn_i serta kecacatan penderma luar di dalam kawasan susutan. Ia disusuli dengan peningkatan dalam ketumpatan perangkap L3 (Sistem 2) dan L4 (Sistem 3) yang dikaitkan dengan pengionan aras tengah jurang yang dirangsang oleh Co dan Mn.

Kesimpulannya, kemerosotan seramik varistor ZnO berasaskan Pr_6O_{11} yang terdop dengan oksida logam peralihan (Co_3O_4, MnO_2 atau Cr_2O_3) dan diterbitkan daripada teknik pengejelan sitrat terubahsuai oleh kerana tekanan berpanjangan medan elektrik dan suhu tinggi adalah kesan langsung kepada keruntuhan Sawar Schottky Ganda dua. Mekanisme kemerosotan ditentukan oleh proses-proses pengelektrohijrahan dan nyahjerapan oksigen yang didorong oleh perubahan kimia dan elektronik berpusat di antaramuka sempadan butir.

© COPYRIGHT UPM

ACKNOWLEDGEMENTS

In the name of Allah, the Most Beneficent, the Most Merciful

All praise be to Allah for His blessings and the strength to continue firmly on this rocky road of doctoral journey. First and foremost, I would like to express my sincerest appreciation to my principal supervisor, Professor Dr. Azmi bin Zakaria for his supervision, constant guidance and knowledge towards the completion of my thesis. I am truly grateful to my co-supervisors, Assoc. Professor Dr. Mansor Hashim and Dr. Md Mahmudur Rahman for their constructive comments and thoughtful suggestions.

I wish to acknowledge Ministry of Higher Education Malaysia for the provision of funding to support this project under Research University Grant Scheme (RUGS) and financial assistance under SLAB scheme within the duration of my doctoral studies. A special recognition is also dedicated to Universiti Malaysia Terengganu for granting my study leave, thus opening the opportunity for improvement of my career prospects. A special credits expressed to Faculty of Science, Institute of Advanced Technology and Institute of Bioscience at Universiti Putra Malaysia for research facilities, conducive learning environment, academic and technical supports.

My truthful thankfulness to my fellow labmates Dr. Zahid Rizwan, Dr. Mohd Sabri Bin Mohd Ghazali, Dr. Munir Noroozi, Atefeh Jafari, Masoumeh Dorraj and Maryam Moosavi for their supports and friendship. Last but never least, I owe a debt of gratitude to my dearest family who endlessly support and pray for my success especially my parents, Wan Abdullah @ Wan Abd Rahman bin Wan Ab. Hamid and Napisah binti Yazziz. I am indebted to my husband, Mohd Ariff bin Isa and my dearest children, Mirza Raimi and Afiah Insyirah a million times for their patience, sacrifices and love. They truly are the source of my motivation and inspiration to successfully accomplish this doctoral thesis.

© COPYRIGHT UPM

I certify that a Thesis Examination Committee has met on 22nd August 2014 to conduct the final examination of Wan Rafizah Binti Wan Abdullah @ Wan Abd. Rahman on her thesis entitled "Degradation Phenomena in Praseodymium Oxide-Based Zinc Oxide Varistor Ceramics Derived Through Modified Citrate Technique" in accordance with the Universities and University Colleges Act 1971 and the Constitution of the Universiti Putra Malaysia [P.U.(A) 106] 15 March 1998. The Committee recommends that the student be awarded the of Doctor of Philosophy.

Members of the Thesis Examination Committee were as follows:

Mohd Nizar bin Hamidon, PhD
Associate Professor
Faculty of Engineering
Universiti Putra Malaysia
(Chairman)

Abdul Halim bin Shaari, PhD
Professor
Faculty of Science
Universiti Putra Malaysia
(Internal Examiner)

Halimah binti Mohamed Kamari, PhD
Associate Professor
Faculty of Science
Universiti Putra Malaysia
(Internal Examiner)

Wan Ping Chen, PhD
Professor
Wuhan University
China
(External Examiner)

NORITAH OMAR, PhD
Associate Professor and Deputy Dean
School of Graduate Studies
Universiti Putra Malaysia

Date:19 September 2014

© COPYRIGHT UPM

This thesis was submitted to the Senate of Universiti Putra Malaysia and has been accepted as fulfilment of the requirement for the degree of Doctor of Philosophy**.** The members of the Supervisory Committee were as follows:

Azmi Bin Zakaria, PhD
Professor
Faculty of Science
Universiti Putra Malaysia
(Chairman)

Mansor Hashim, PhD
Associate Professor
Faculty of Science
Universiti Putra Malaysia
(Member)

Mahmudur Rahman, PhD
Lecturer
Faculty of Science
Universiti Putra Malaysia
(Member)

BUJANG BIN KIM HUAT, PhD
Professor and Dean
School of Graduate Studies
Universiti Putra Malaysia

Date:

© COPYRIGHT UPM

Declaration by graduate student

I hereby confirm that:

- this thesis is my original work;
- quotations, illustrations and citations have been duly referenced;
- this thesis has not been submitted previously or concurrently for any other degree at any other institutions;
- intellectual property from the thesis and copyright of thesis are fully-owned by Universiti Putra Malaysia, as according to Universiti Putra Malaysia (Research) Rules 2012;
- written permission must be obtained from supervisor and the office of Deputy Vice-Chancellor (Research and Innovation) before thesis is published (in the form of written, printed or in electronic form) including books, journals, modules, proceedings, popular writings, seminar papers, manuscripts, posters, reports, lecture notes, learning modules or any other materials as stated in the Universiti Putra Malaysia (Research) Rules 2012;
- there is no plagiarism or data falsification/fabrication in the thesis, and scholarly integrity is upheld as according to the Universiti Putra Malaysia (Graduate Studies) Rules 2003 (Revision 2012-2013) and the Universiti Putra Malaysia (Research) Rules 2012. The thesis has undergone plagiarism detection software.

Signature: 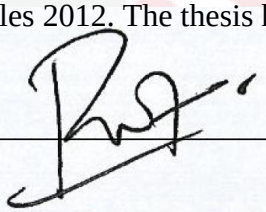 Date: 17th October 2014

Name and Matric No.:Wan Rafizah binti Wan Abdullah @ Wan Abd. Rahman, GS27520

© COPYRIGHT UPM

Declaration by Members of Supervisory Committee

This is to confirm that:

- the research conducted and the writing of this thesis was under our supervision;
- supervision responsibilities as stated in the Universiti Putra Malaysia (Graduate Studies) Rules 2003 (Revision 2012-2013) are adhered to.

Signature: _____

Name of Chairman of Supervisory Committee: Azmi Zakaria, PhD

DR. AZMI ZAKARIA
Profesor
Jabatan Fizik
Fakulti Sains
Universiti Putra Malaysia
43400 UPM Serdang

Signature: _____

Name of Member of Supervisory Committee: Mansor Hashim, PhD

PROF MADYA DR. MANSOR HASHIM
Ketua Program
Laboratori Sintesis dan Pencirian Bahan
Institut Teknologi Maju
Universiti Putra Malaysia
43400 Serdang, Selangor

Signature: _____

Name of Member of Supervisory Committee: Md Mahmudur Rahman, PhD

DR. MD. MAHMUDUR RAHMAN
Pensyarah Kanan
Jabatan Fizik
Fakulti Sains
Universiti Putra Malaysia
43400 UPM Serdang, Selangor

TABLE OF CONTENTS

		Page
ABSTRACT		i
ABSTRAK		iv
ACKNOWLEDGEMENTS		vii
APPROVAL		viii
DECLARATION		x
LIST OF TABLES		xvi
LIST OF FIGURES		xxii
LIST OF ABBREVIATIONS		xxxii
LIST OF SYMBOLS		xxxiii
CHAPTER		
1	**INTRODUCTION**	
	1.0 Introduction	1
	1.1 Research Background	1
	1.1.1 Overview of Metal Oxide Varistor Development	1
	1.1.2 Zinc Oxide Varistors	2
	1.1.3 Electrical Nonlinearity	4
	1.1.4 Low-voltage Varistors	6
	1.1.5 Praseodymium Oxide Based ZnO Varistors	8
	1.1.6 Varistor Degradation	8
	1.2 Problem Statements	9
	1.3 Research Objectives	10
	1.4 Research Scopes	11
	1.5 Research Significance	12
	1.6 Thesis Organization	12
2	**LITERATURE REVIEW**	
	2.0 Introduction	14
	2.1 Historical Development of Nonlinear Varistors	14
	2.2 Development of Varistor Microstructure	14
	2.2.1 Grain	15
	2.2.2 Grain Boundary	16
	2.2.3 Triple Point	17
	2.2.4 Spinel and Pyrochlore Phases	17
	2.2.5 Pores	18
	2.3 Roles of Dopants	18
	2.3.1 Varistor Forming Oxides	18
	2.3.2 Varistor Enhancers	23
	2.3.3 Varistor Highlighters	24
	2.4 Degradation	25
	2.4.1 Effects of Degradation	25

© COPYRIGHT UPM

2.4.2 Factors Accelerating Degradation 26
2.4.3 Restoration of Degradation 27
2.5 Deep Level Transients Spectroscopy Technique 28
2.5.1 Deep level Characteristics of ZnO Varistors 28
2.5.2 Degradation Analysis Using DLTS 31

3 THEORY
3.0 Introduction 33
3.1 Intrinsic Properties of ZnO 33
3.2 The Block Model 34
3.3 Microstructure-electrical Models 35
3.3.1 Double Schottky Barrier Model 36
3.3.2 Charged Grain Boundary Model 37
3.3.3 Atomic Defect Model 38
3.3.4 Avalanche Breakdown Model 39
3.4 Degradation Mechanisms 40
3.4.1 Electromigration 40
3.4.2 Oxygen Desorption 42
3.5 Deep Level Theory 42
3.5.1 Definition and Characteristics 42
3.5.2 Capacitance of Schottky Barrier Diodes 43
3.5.3 Electron Capture and Emission 44
3.5.4 Basic Measurement Technique 45
3.5.5 Deep-level Parameters 48

4 METHODOLOGY
4.0 Introduction 49
4.1 Research Design 49
4.2 Materials Selection 49
4.2.1 ZnO 51
4.2.2 Dopant Precursors 51
4.2.3 Complexing Agent 52
4.2.4 Other Chemicals 53
4.3 Ceramic Formulations 53
4.4 Preparation of Precursor Powder 54
4.4.1 Citrate Complexation Reaction 55
4.4.2 Mixing and Drying 56
4.4.3 Calcination 56
4.4.4 Preparation of Precursor Powder for Binary Doping System 58
4.5 Preparation of Varistor Ceramics 59
4.5.1 Pellet Pressing 59
4.5.2 Sintering 60
4.6 Characterization Methods 61
4.6.1 XRD 61
4.6.2 FESEM 62

© COPYRIGHT UPM

4.6.3 EDX 62
4.6.4 Grain Size Measurement 63
4.6.5 Density Measurement 63
4.6.6 J-E Characteristics Measurement 64
4.6.7 DC Degradation Testing 64
4.6.8 DLTS Measurement 66

5 RESULTS AND DISCUSSION
5.0 Introduction 71
5.1 System 1 71
5.1.1 Effects of Pr_6O_{11} Contents on Microstructure and Nonlinear Properties 71
5.1.2 Effects of Sintering Temperature on Microstructure and Nonlinear Properties 83
5.1.3 Effects of Sintering Time on Microstructure and Nonlinear Properties 90
5.1.4 Effects of DC electrical Field and Thermal Stresses on Nonlinear Properties 98
5.1.5 The Influence of Deep Levels on Degradation Behaviour 104
5.1.6 Summary of Findings 106
5.2 System 2 109
5.2.1 Effects of Co_3O_4 Contents on Microstructure and Nonlinear Properties 109
5.2.2 Effects of Sintering Temperature on Microstructure and Nonlinear Properties 118
5.2.3 Effects of Sintering Time on Microstructure and Nonlinear Properties 125
5.2.4 Effects of DC electrical Field and Thermal Stresses on Nonlinear Properties 132
5.2.5 The Influence of Deep Levels on Degradation Behaviour 137
5.2.6 Summary of Findings 139
5.3 System 3 142
5.3.1 Effects of MnO_2 Contents on Microstructure and Nonlinear Properties 142
5.3.2 Effects of Sintering Temperature on Microstructure and Nonlinear Properties 152
5.3.3 Effects of Sintering Time on Microstructure and Nonlinear Properties 160
5.3.4 Effects of DC Electrical Field and Thermal Stresses on Nonlinear Properties 167
5.3.5 The Influence of Deep Levels on Degradation Behaviour 173
5.3.6 Summary of Findings 175

© COPYRIGHT UPM

5.4 System 4 177
5.4.1 Effects of Cr_2O_3 Contents on Microstructure and Nonlinear Properties 177
5.4.2 Effects of Sintering Temperature on Microstructure and Nonlinear Properties 186
5.4.3 Effects of Sintering Time on Microstructure and Nonlinear Properties 193
5.4.4 Effects of DC Electrical Field and Thermal Stresses on Nonlinear Properties 200
5.4.5 The Influence of Deep Levels on Degradation Behaviour 206
5.4.6 Summary of Findings 208

6 GENERAL CONCLUSIONS AND RECOMMENDATIONS FOR FUTURE RESEARCH
6.0 Introduction 211
6.1 General Conclusions 211
6.2 Recommendations for Future Research 213

REFERENCES 214
APPENDICES 232
BIODATA OF STUDENT 253
LIST OF PUBLICATIONS 254

© COPYRIGHT UPM

LIST OF TABLES

Table		Page
2.1	Comparison of various varistor former materials in ZnO based varistors	19
2.2	Previous selected studies on Pr_6O_{11} based ZnO varistor ceramics	21
2.3	Deep-levels in ZnO varistor ceramics reported in previous studies	29
3.1	Characteristics of electron and hole traps in a semiconductor	43
4.1	Physical and chemical properties of ZnO	51
4.2	Physical and chemical properties of Pr and Co acetates	52
4.3	Physical and chemical properties of Mn and Cr acetates	52
4.4	Physical and chemical properties of citric acid	52
4.5	Varistor ceramic systems and their corresponding nominal formulations	53
4.6	Molar ratio of citric acid to metal salts	58
4.7	Sintering conditions applied in preparation of varistor ceramics	60
4.8	Settings for DLTS measurement	69
5.1	The phase identification in ZnO ceramics doped with different Pr_6O_{11} contents	72
5.2	The *d*-spacings of ZnO crystal with respect to Pr_6O_{11} contents	73
5.3	The average lattice constants of ZnO crystal with respect to Pr_6O_{11} contents	73
5.4	Average grain size and average relative density of ZnO varistor ceramics with different Pr_6O_{11} contents and sintered at 1250 ^oC for 1 h	77
5.5	J-E characteristic parameters of Pr_6O_{11} doped ZnO varistor ceramics with different Pr_6O_{11} contents	79

© COPYRIGHT UPM

5.6	The phase identification in Pr_6O_{11} doped ZnO ceramics sintered at different sintering temperatures	84
5.7	The *d*-spacings of ZnO crystal with respect to sintering temperature for Pr_6O_{11} doped ZnO ceramics	84
5.8	The average lattice constants of ZnO crystal with respect to sintering temperature for Pr_6O_{11} doped ZnO ceramics	84
5.9	Average grain size and average relative density of ZnO varistor ceramics doped with 0.2 mol% Pr_6O_{11} and sintered at different sintering temperatures for 1 h	86
5.10	J-E characteristic parameters of Pr_6O_{11} doped ZnO varistor ceramics sintered at different sintering temperatures	88
5.11	The phase identification in Pr_6O_{11} doped ZnO ceramics with different sintering time	91
5.12	The *d*-spacings of ZnO crystal with respect to sintering time for Pr_6O_{11} doped ZnO ceramics	92
5.13	The average lattice constants of ZnO crystal with respect to sintering time for Pr_6O_{11} doped ZnO ceramics	92
5.14	Average grain size and average relative density of ZnO varistor ceramics doped with 0.2 mol% Pr_6O_{11} and sintered at 1250 ^oC for different sintering time	94
5.15	J-E characteristic parameters of Pr_6O_{11} doped ZnO varistor ceramics at different sintering time	96
5.16	J-E characteristics of initial and degraded Pr_6O_{11} doped ZnO varistor ceramics	100
5.17	Comparison of deep level properties for electron traps in initial and degraded ZnO varistor ceramics doped with 0.2 mol% Pr_6O_{11} and sintered at 1250 ^oC for 1 h	105
5.18	The phase identification in Pr_6O_{11} based ZnO ceramics doped with different Co_3O_4 contents	110
5.19	The *d*-spacings of ZnO crystal with respect to Co_3O_4 contents	111
5.20	The average lattice constants of ZnO crystal with respect to Co_3O_4 contents	111

© COPYRIGHT UPM

5.21	Average grain size and average relative density of Pr_6O_{11} based ZnO varistor ceramics doped with different Co_3O_4 contents and sintered at 1250 ^oC for 1 h	114
5.22	J-E characteristic parameters of Pr_6O_{11} based ZnO varistor ceramics doped with different Co_3O_4 contents	117
5.23	The phase identification in Pr_6O_{11} based ZnO ceramics doped with Co_3O_4 and sintered at different sintering temperatures	119
5.24	The *d*-spacings of ZnO crystal with respect to sintering temperature for Pr_6O_{11} based ZnO ceramics doped with Co_3O_4	120
5.25	The average lattice constants of ZnO crystal with respect to sintering temperature for Pr_6O_{11} based ZnO ceramics doped with Co_3O_4	120
5.26	Average grain size and average relative density of Pr_6O_{11} based ZnO varistor ceramics doped with 1.0 mol% Co_3O_4 and sintered at different sintering temperatures for 1 h	122
5.27	J-E characteristic parameters of Pr_6O_{11} based ZnO varistor ceramics doped with Co_3O_4 and sintered at different sintering temperatures	124
5.28	The phase identification in Pr_6O_{11} based ZnO ceramics doped with Co_3O_4 and sintered for different sintering time	126
5.29	The *d*-spacings of ZnO crystal with respect to sintering time for Pr_6O_{11} based ZnO ceramics doped with Co_3O_4	127
5.30	The average lattice constants of ZnO crystal with respect to sintering time for Pr_6O_{11} based ZnO ceramics doped with Co_3O_4	127
5.31	Average grain size and average relative density of Pr_6O_{11} based ZnO varistor ceramics doped with 1.0 mol% Co_3O_4 and sintered at 1250 ^oC for different sintering time	129
5.32	J-E characteristic parameters of Pr_6O_{11} based ZnO varistor ceramics doped with Co_3O_4 and sintered for different sintering time	130
5.33	J-E characteristics of initial and degraded Pr_6O_{11} based ZnO varistor ceramics doped with Co_3O_4	134
5.34	Comparison of deep level properties for electron traps in initial and degraded Pr_6O_{11} based ZnO varistors ceramic doped with 1.0 mol% Co_3O_4 and sintered at 1250 ^oC for 1 h	139

© COPYRIGHT UPM

5.35	The phase identification in Pr_6O_{11} based ZnO ceramics doped with different MnO_2 contents	143
5.36	The *d*-spacings of ZnO crystal with respect to MnO_2 contents	143
5.37	The average lattice constants of ZnO crystal with respect to MnO_2 contents	144
5.38	Average grain size and average relative density of Pr_6O_{11} based ZnO varistor ceramics doped with different MnO_2 contents and sintered at 1250 ^oC for 1 h	147
5.39	J-E characteristic parameters of Pr_6O_{11} based ZnO varistor ceramics doped with different MnO_2 contents	149
5.40	The phase identification in Pr_6O_{11} based ZnO ceramics doped with MnO_2 and sintered at different sintering temperatures	153
5.41	The *d*-spacings of ZnO crystal with respect to sintering temperature for Pr_6O_{11} based ZnO ceramics doped with MnO_2	154
5.42	The average lattice constants of ZnO crystal with respect to sintering temperature for Pr_6O_{11} based ZnO ceramics doped with MnO_2	154
5.43	Average grain size and average density of Pr_6O_{11} based ZnO varistor ceramics doped with 0.4 mol% MnO_2 and sintered at different sintering temperatures for 1 h	155
5.44	J-E characteristic parameters of Pr_6O_{11} based ZnO varistor ceramics doped with MnO_2 and sintered at different sintering temperatures	157
5.45	The phase identification in Pr_6O_{11} based ZnO ceramics doped with MnO_2 and sintered at different sintering time	161
5.46	The *d*-spacings of ZnO phase with respect to sintering time for Pr_6O_{11} based ZnO ceramics doped with MnO_2	161
5.47	The average lattice constants of ZnO crystal with respect to sintering time for Pr_6O_{11} based ZnO ceramics doped with MnO_2	162
5.48	Average grain size and average density of Pr_6O_{11} based ZnO varistor ceramics doped with 0.4 mol% MnO_2 and sintered at 1250 ^oC for different sintering time	163

© COPYRIGHT UPM

5.49	J-E characteristic parameters of Pr_6O_{11} based ZnO varistor ceramics doped with MnO_2 and sintered for different sintering time	165
5.50	J-E characteristics of initial and degraded Pr_6O_{11} based ZnO varistor ceramics doped with MnO_2	169
5.51	Comparison of deep level properties for electron traps in initial and degraded Pr_6O_{11} based ZnO varistors doped with 0.4 mol% MnO_2 and sintered at 1250 ^oC for 1 h	174
5.52	The phase identification in Pr_6O_{11} based ZnO ceramics doped with different Cr_2O_3 contents	178
5.53	The *d*-spacings of ZnO crystal with respect to Cr_2O_3 contents	179
5.54	The average lattice constants of ZnO crystal with respect to Cr_2O_3 contents	179
5.55	Average grain size and average density of Pr_6O_{11} based ZnO varistor ceramics doped with different Cr_2O_3 contents and sintered at 1250 ^oC for 1 h	182
5.56	J-E characteristic parameters of Pr_6O_{11} based ZnO varistor ceramics doped with different Cr_2O_3 contents	185
5.57	The phase identification in Pr_6O_{11} based ZnO ceramics doped with Cr_2O_3 and sintered at different sintering temperatures	187
5.58	The *d*-spacings of ZnO crystal with respect to sintering temperature for Pr_6O_{11} based ZnO ceramics doped with Cr_2O_3	188
5.59	The average lattice constants of ZnO crystal with respect to sintering temperature for Pr_6O_{11} based ZnO ceramics doped with Cr_2O_3	188
5.60	Average grain size and average density of Pr_6O_{11} based ZnO varistor ceramics doped with 0.6 mol% Cr_2O_3 and sintered at different sintering temperatures for 1 h	190
5.61	J-E characteristic parameters of Pr_6O_{11} based ZnO varistor ceramics doped with Cr_2O_3 and sintered at different sintering temperatures	192
5.62	The phase identification in Pr_6O_{11} based ZnO ceramics doped with Cr_2O_3 and sintered at different sintering time	194
5.63	The *d*-spacings of ZnO crystal with respect to sintering time for Pr_6O_{11} based ZnO ceramics doped with Cr_2O_3	195

© COPYRIGHT UPM

5.64	The average lattice constants of ZnO crystal with respect to sintering time for Pr_6O_{11} based ZnO ceramics doped with Cr_2O_3	195
5.65	Average grain size and average density of Pr_6O_{11} based ZnO varistor ceramics doped with 0.6 mol% Cr_2O_3 and sintered at 1250 ^oC for different sintering time	197
5.66	J-E characteristic parameters of Pr_6O_{11} based ZnO varistor ceramics doped with Cr_2O_3 and sintered for different sintering time	198
5.67	J-E characteristics of initial and degraded Pr_6O_{11} based ZnO varistor ceramics doped with Cr_2O_3	202
5.68	Comparison of deep level properties for electron traps in initial and degraded Pr_6O_{11} based ZnO varistors doped with 0.6 mol% Cr_2O_3 and sintered at 1250 ^oC for 1 h	207

© COPYRIGHT UPM

LIST OF FIGURES

Figure		Page
1.1	Typical placement of varistor in a circuit	1
1.2	A typical construction of a ZnO varistor device	3
1.3	Typical J-E characteristic of a ZnO varistor	4
1.4	Variation in nonlinear coefficient with current density	6
2.1	Typical grain microstructure of ZnO varistor ceramic	15
2.2	Types of grain boundary microstructures in ZnO varistor ceramics	16
3.1	A wurtzitic ZnO crystal stucture	34
3.2	The Block Model	35
3.3	Double Schottky Barrier Model	36
3.4	Formation of potential barrier at a grain boundary	37
3.5	Atomic Defect Model	39
3.6	Breakdown phenomenon according to Avalanche Breakdown Model	40
3.7	Barrier deformation that is attributed to (a) diffusion of interstitial Zn and (b) chemical reaction occurring at grain boundary during energization	41
3.8	Restoration of barrier that is attributed to (a) ionization of Zn at interface and (b) diffusion of interstitial Zn to depletion region during de-energization	42
3.9	The bending of energy bands for an *n*-type Schottky barrier diode	43
3.10	Electron emission and capture process according to Shockley Read Hall kinetics	44
3.11	Electron injection process	45
3.12	Determination of the capacitance transient after pulse filling	46

© COPYRIGHT UPM

3.13	The temperature dependence of DLTS signal	47
4.1	Experimental design	50
4.2	List of raw materials	50
4.3	Molecular structure of citric acid	53
4.4	Precursor powder preparation for single doping system	55
4.5	FESEM micrograph of precursor powder containing calcined and Pr-coated ZnO particles at 100 000 times magnification	57
4.6	Precursor powder preparation for binary doping system	58
4.7	TEM images of Pr and Cr gel coated ZnO powder after calcination	59
4.8	Preparation of precursor pellet	60
4.9	Schematic diagram of DC degradation test setup	65
4.10	SemiLab's DLS-83D system	67
4.11	Schematic diagram of electrical connection for DLTS measurement	68
5.1	XRD patterns of Pr_6O_{11} based ZnO varistor ceramics doped with different Pr_6O_{11} contents and sintered at 1250 ^oC for 1 h	72
5.2	FESEM images for grain structure of ZnO varistor ceramics doped with different Pr_6O_{11} contents and sintered at 1250 ^oC for 1 h	74
5.3	EDX spectra of the (a) grain, (b) grain boundary and (c) triple point regions on ZnO ceramics doped with Pr_6O_{11} and sintered at 1250 ^oC for 1 h	76
5.4	Average grain size and average relative density with Pr_6O_{11} contents	77
5.5	J-E curves of ZnO varistor ceramics doped with different Pr_6O_{11} contents and sintered at 1250 ^oC for 1 h	79
5.6	Variations of (a) nonlinear coefficient, (b) breakdown field and (c) leakage current density of ZnO varistor ceramics doped with different Pr_6O_{11} contents	80

© COPYRIGHT UPM

5.7	Average voltage per grain boundary and potential barrier height in pre-breakdown region of Pr_6O_{11} based ZnO varistor ceramics doped with different Pr_6O_{11} contents	82
5.8	XRD patterns of ZnO varistor ceramics doped with 0.2 mol% Pr_6O_{11} and sintered at different sintering temperatures for 1 h	83
5.9	FESEM images for grain structure of ZnO varistor ceramics doped with 0.2 mol% Pr_6O_{11} and sintered at different sintering temperatures for 1 h	85
5.10	Average grain size and average relative density with sintering temperature for Pr_6O_{11} doped ZnO ceramics	87
5.11	J-E curves of ZnO varistor ceramics doped with 0.2 mol% Pr_6O_{11} and sintered at different sintering temperatures for 1 h	88
5.12	Variations of (a) nonlinear coefficient, (b) breakdown field and (c) leakage current density of Pr_6O_{11} based ZnO varistor ceramics sintered at different sintering temperatures	89
5.13	Average voltage per grain boundary and potential barrier height in pre-breakdown region of Pr_6O_{11} based ZnO varistor ceramics sintered at different sintering temperatures	90
5.14	XRD patterns of ZnO varistor ceramics doped with 0.2 mol% Pr_6O_{11} and sintered at 1250 ^oC for different sintering time	91
5.15	FESEM images for grain structure of ZnO varistor ceramics doped with 0.2 mol% Pr_6O_{11} and sintered at 1250 ^oC for different sintering time	93
5.16	Average grain size and average relative density with sintering time for Pr_6O_{11} doped ZnO ceramics	94
5.17	J-E curves of ZnO varistor ceramics doped with 0.2 mol% Pr_6O_{11} and sintered at 1250 ^oC for different sintering time	95
5.18	Variations of (a) nonlinear coefficient, (b) breakdown field and (c) leakage current density of Pr_6O_{11} based ZnO varistor ceramics sintered for different sintering time	96
5.19	Average voltage per grain boundary and potential barrier height in pre-breakdown region of Pr_6O_{11} based ZnO varistor ceramics sintered for different sintering time	97

© COPYRIGHT UPM

5.20	Comparison of J-E curves for initial and degraded ZnO varistor ceramics doped with 0.2 mol% Pr_6O_{11} and sintered at 1250 ^oC for 1 h	98
5.21	Current creep in Pr_6O_{11} doped ZnO varistors during stressing time	99
5.22	The effect of DC degradation on average voltage per grain boundary and potential barrier height for Pr_6O_{11} doped ZnO ceramics	101
5.23	Temperature-dependent coefficient for leakage current of ZnO varistor ceramics doped with 0.2 mol% Pr_6O_{11} and sintered at 1250 ^oC for 1 h	102
5.24	Comparison of (a) the average relative density, (b) the initial leakage current density and (c) degradation rate coefficient, K_T with respect to Pr_6O_{11} contents for System 1 ceramics	103
5.25	DLTS spectra of initial and degraded ZnO varistor ceramics doped with 0.2 mol% Pr_6O_{11} and sintered at 1250 ^oC for 1 h	104
5.26	XRD patterns of Pr_6O_{11} based ZnO varistor ceramics doped with different Co_3O_4 contents and sintered at 1250 ^oC for 1 h	109
5.27	FESEM images for grain structure of Pr_6O_{11} based ZnO varistor ceramics doped with different Co_3O_4 contents and sintered at 1250 ^oC for 1 h	112
5.28	EDX spectra of the (a) grain, (b) grain boundary and (c) triple point regions on Pr_6O_{11} based ZnO ceramics doped with Co_3O_4 and sintered at 1250 ^oC for 1 h	113
5.29	Average grain size and average relative density with Co_3O_4 contents	115
5.30	J-E curves of Pr_6O_{11} based ZnO varistor ceramics doped with different Co_3O_4 contents and sintered at 1250 ^oC for 1 h	116
5.31	Variations of (a) nonlinear coefficient, (b) breakdown field and (c) leakage current density of Pr_6O_{11} based ZnO varistor ceramics doped with different Co_3O_4 contents	117
5.32	Average voltage per grain boundary and potential barrier height in prebreakdown region of Pr_6O_{11} based ZnO varistor ceramics doped with different Co_3O_4 contents	118

© COPYRIGHT UPM

5.33	XRD patterns of Pr_6O_{11} based ZnO varistor ceramics doped with 1.0 mol% Co_3O_4 and sintered at different sintering temperatures for 1 h	119
5.34	FESEM images for grain structure of Pr_6O_{11} based ZnO varistor ceramics doped with 1.0 mol% Co_3O_4 and sintered at different sintering temperatures for 1 h	121
5.35	Average grain size and average relative density with sintering temperature for Pr_6O_{11} based ZnO ceramics doped with Co_3O_4	122
5.36	J-E curves of Pr_6O_{11} based ZnO varistor ceramics doped with 1.0 mol% Co_3O_4 and sintered at different sintering temperatures for 1 h	123
5.37	Variations of (a) nonlinear coefficient, (b) breakdown field and (c) leakage current density of Pr_6O_{11} based ZnO varistor ceramics doped with Co_3O_4 and sintered at different sintering temperatures	124
5.38	Average voltage per grain boundary and potential barrier height in pre-breakdown region of Pr_6O_{11} based ZnO varistor ceramics doped with Co_3O_4 and sintered at different sintering temperatures	125
5.39	XRD patterns of Pr_6O_{11} based ZnO varistor ceramics doped with 1.0 mol% Co_3O_4 and sintered at 1250 ^oC for different sintering time	126
5.40	FESEM images for grain structure of Pr_6O_{11} based ZnO varistor ceramics doped with 1.0 mol% Co_3O_4 and sintered at 1250 ^oC for different sintering time	128
5.41	Average grain size and average relative density with sintering time for Pr_6O_{11} based ZnO ceramics doped with Co_3O_4	129
5.42	J-E curves of Pr_6O_{11} based ZnO varistor ceramics doped with 1.0 mol% Co_3O_4 and sintered at 1250 ^oC for different sintering time	130
5.43	Variations of (a) nonlinear coefficient, (b) breakdown field and (c) leakage current density of Pr_6O_{11} based ZnO varistor ceramics doped with Co_3O_4 and sintered for different sintering time	131
5.44	Average voltage per grain boundary and potential barrier height in pre-breakdown region of Pr_6O_{11} based ZnO varistor ceramics doped with Co_3O_4 and sintered for different sintering time	132

© COPYRIGHT UPM

5.45 Comparison of J-E curves for initial and degraded Pr_6O_{11} based ZnO varistor ceramics doped with 1.0 mol% Co_3O_4 and sintered at 1250 ^oC for 1 h 133

5.46 Current creep in Pr_6O_{11} based ZnO varistor ceramics doped with Co_3O_4 during stressing time 134

5.47 The effect of DC degradation on average voltage per grain boundary and potential barrier height for Pr_6O_{11} based ZnO ceramics doped with Co_3O_4 135

5.48 Temperature-dependent coefficient, k_L for leakage current of Pr_6O_{11} based ZnO varistor ceramics doped with 1.0 mol% Co_3O_4 and sintered at 1250 ^oC for 1 h 136

5.49 Comparison of (a) the average relative density, (b) the initial leakage current density and (c) degradation rate coefficient, K_T with respect to Co_3O_4 contents for System 2 ceramics 137

5.50 DLTS spectra of initial and degraded Pr_6O_{11} based ZnO varistor ceramics doped with 1.0 mol% Co_3O_4 and sintered at 1250 ^oC for 1 h 138

5.51 XRD patterns of Pr_6O_{11} based ZnO varistor ceramics doped with different MnO_2 contents and sintered at 1250 ^oC for 1 h 142

5.52 FESEM images for grain structure of Pr_6O_{11} based ZnO varistor ceramics doped with different MnO_2 contents and sintered at 1250 ^oC for 1 h 145

5.53 EDX spectra of the (a) grain, (b) grain boundary and (c) triple point regions on Pr_6O_{11} based ZnO varistor ceramics doped with MnO_2 and sintered at 1250 ^oC for 1 h 146

5.54 Average grain size and average relative density with MnO_2 contents 148

5.55 J-E curves of Pr_6O_{11} based ZnO varistor ceramics doped with different MnO_2 contents and sintered at 1250 ^oC for 1 h 149

5.56 Variations of (a) nonlinear coefficient, (b) breakdown field and (c) leakage current density of Pr_6O_{11} based ZnO varistor ceramics doped with different MnO_2 contents 150

5.57 Average voltage per grain boundary and potential barrier height in pre-breakdown region of Pr_6O_{11} based ZnO varistor ceramics doped with different MnO_2 contents 151

© COPYRIGHT UPM

5.58 XRD patterns of Pr_6O_{11} based ZnO varistor ceramics doped with 0.4 mol% MnO_2 and sintered at different sintering temperatures for 1 h 152

5.59 FESEM images for the grain structure of Pr_6O_{11} based ZnO varistor ceramics doped with 0.4 mol% MnO_2 and sintered at different sintering temperatures for 1 h 155

5.60 Average grain size and average relative density with sintering temperatures for Pr_6O_{11} based ZnO ceramics doped with MnO_2 156

5.61 J-E curves of Pr_6O_{11} based ZnO varistor ceramics doped with 0.4 mol% MnO_2 and sintered at different sintering temperatures for 1 h 157

5.62 Variations of (a) nonlinear coefficient, (b) breakdown field and (c) leakage current density of Pr_6O_{11} based ZnO varistor ceramics doped with MnO_2 and sintered at different sintering temperatures 158

5.63 Average voltage per grain boundary and potential barrier height in pre-breakdown region of Pr_6O_{11} based ZnO varistor ceramics doped with MnO_2 and sintered at different sintering temperatures 159

5.64 XRD patterns of Pr_6O_{11} based ZnO varistor ceramics doped with 0.4 mol % MnO_2 and sintered at 1250 ^oC for different sintering time 160

5.65 FESEM images for the grain structure of Pr_6O_{11} based ZnO varistor ceramics doped with 0.4 mol % MnO_2 and sintered at 1250 ^oC for different sintering time 162

5.66 Average grain size and average relative density with sintering time for Pr_6O_{11} based ZnO ceramics doped with MnO_2 164

5.67 J-E curves of Pr_6O_{11} based ZnO varistor ceramics doped with 0.4 mol % MnO_2 and sintered at 1250 ^oC for different sintering time 165

5.68 Variations of (a) nonlinear coefficient, (b) breakdown field and (c) leakage current density of Pr_6O_{11} based ZnO varistor ceramics doped with MnO_2 and sintered for different sintering time 166

5.69 Average voltage per grain boundary and potential barrier height in pre-breakdown region of Pr_6O_{11} based ZnO varistor ceramics doped with MnO_2 and sintered for different sintering time 167

© COPYRIGHT UPM

5.70 Comparison of J-E curves for initial and degraded Pr_6O_{11} based ZnO varistor ceramics doped with 0.4 mol% MnO_2 and sintered at 1250 ^oC for 1 h 168

5.71 Current creep in Pr_6O_{11} based ZnO varistor ceramics doped with MnO_2 during stressing time 169

5.72 The effect of DC degradation on average voltage per grain boundary and potential barrier height for Pr_6O_{11} based ZnO ceramics doped with MnO_2 170

5.73 Temperature-dependent coefficient, k_L for leakage current of Pr_6O_{11} based ZnO varistor ceramics doped with 0.4 mol% MnO_2 and sintered at 1250 ^oC for 1 h 171

5.74 Comparison of (a) the average relative density, (b) the initial leakage current density and (c) degradation rate coefficient, K_T with respect to MnO_2 contents for System 3 ceramics 172

5.75 DLTS spectra of initial and degraded Pr_6O_{11} based ZnO varistor ceramics doped with 0.4 mol% MnO_2 and sintered at 1250 ^oC for 1 h 173

5.76 XRD patterns of Pr_6O_{11} based ZnO varistor ceramics doped with different Cr_2O_3 contents and sintered at 1250 ^oC for 1 h 177

5.77 FESEM images for grain structure of Pr_6O_{11} based ZnO varistor ceramics doped with different Cr_2O_3 and sintered at 1250 ^oC for 1 h 180

5.78 EDX spectra of the (a) grain, (b) grain boundary and (c) triple point regions on Pr_6O_{11} based ZnO varistor ceramics doped with Cr_2O_3 and sintered at 1250 ^oC for 1 h 181

5.79 Average grain size and average relative density with Cr_2O_3 contents 183

5.80 J-E curves of Pr_6O_{11} based ZnO varistor ceramics doped with different Cr_2O_3 contents and sintered at 1250 ^oC for 1 h 184

5.81 Variations of (a) nonlinear coefficient, (b) breakdown field and (c) leakage current density of Pr_6O_{11} based ZnO varistor ceramics doped with different Cr_2O_3 contents 185

5.82 Average voltage per grain boundary and potential barrier height in pre-breakdown region of Pr_6O_{11} based ZnO varistor ceramics doped with different Cr_2O_3 contents 186

© COPYRIGHT UPM

5.83 XRD patterns of Pr_6O_{11} based ZnO varistor ceramics doped with 0.6 mol% Cr_2O_3 and sintered at different sintering temperatures for 1 h 187

5.84 FESEM images for the grain structure of Pr_6O_{11} based ZnO varistor ceramics doped with 0.6 mol% Cr_2O_3 and sintered at different sintering temperatures for 1 h 189

5.85 Average grain size and average relative density with sintering temperature for Pr_6O_{11} based ZnO ceramics doped with Cr_2O_3 190

5.86 J-E curves of Pr_6O_{11} based ZnO varistor ceramics doped with 0.6 mol% Cr_2O_3 and sintered at different sintering temperatures for 1 h 191

5.87 Variations of (a) nonlinear coefficient, (b) breakdown field and (c) leakage current density of Pr_6O_{11} based ZnO varistor ceramics doped with Cr_2O_3 and sintered at different sintering temperatures 192

5.88 Average voltage per grain boundary and potential barrier height in pre-breakdown region of Pr_6O_{11} based ZnO varistor ceramics doped with Cr_2O_3 and sintered at different sintering temperatures 193

5.89 XRD patterns of Pr_6O_{11} based ZnO varistor ceramics doped with 0.6 mol% Cr_2O_3 and sintered at 1250 ^oC for different sintering time 194

5.90 FESEM images for the grain structure of Pr_6O_{11} based ZnO varistor ceramics doped with 0.6 mol% Cr_2O_3 and sintered at 1250 ^oC for different sintering time 196

5.91 Average grain size and average relative density with sintering time for Pr_6O_{11} based ZnO ceramics doped with Cr_2O_3 197

5.92 J-E curves of Pr_6O_{11} based ZnO varistor ceramics doped with 0.6 mol% Cr_2O_3 and sintered at 1250 ^oC for different sintering time 198

5.93 Variations of (a) nonlinear coefficient, (b) breakdown field and (c) leakage current density of Pr_6O_{11} based ZnO varistor ceramics doped with Cr_2O_3 and sintered for different sintering time 199

5.94 Average voltage per grain boundary and potential barrier height in pre-breakdown region of Pr_6O_{11} based ZnO varistor ceramics doped with Cr_2O_3 and sintered for different sintering time 200

© COPYRIGHT UPM

5.95	Comparison of J-E curves for initial and degraded Pr_6O_{11} based ZnO varistor ceramics doped with 0.6 mol% Cr_2O_3 and sintered at 1250 ^oC for 1 h	201
5.96	Current creep in Pr_6O_{11} based ZnO varistor ceramics doped with Cr_2O_3 during stressing time	202
5.97	The effect of DC degradation on average voltage per grain boundary and potential barrier height	203
5.98	Temperature-dependent coefficient, k_L for leakage current of Pr_6O_{11} based ZnO varistor ceramics doped with 0.6 mol% Cr_2O_3 and sintered at 1250 ^oC for 1 h	204
5.99	Comparison of (a) the average relative density, (b) the initial leakage current density and (c) degradation rate coefficient, K_T with respect to Cr_2O_3 contents for System 4 ceramics	205
5.100	DLTS spectra of initial and degraded Pr_6O_{11} based ZnO varistor ceramics doped with 0.6 mol% Cr_2O_3 and sintered at 1250 ^oC for 1 h	206

© COPYRIGHT UPM

LIST OF ABBREVIATIONS

AC	Alternating current
AES	Auger electron spectroscopy
C-V	Capacitance-voltage
DC	Direct current
DSB	Double Schottky barrier
DLTS	Deep level transient spectroscopy
EDX	Energy dispersive X-ray spectroscopy
ESD	Electrostatic discharge
FESEM	Field emission scanning electron microscopy
FW	Formula weight
HRTEM	High resolution transmission electron microscopy
ICSD	Inorganic crystal structure database
ICTS	Isothermal capacitance transient spectroscopy
I-V	Current-voltage
J-E	Current density - electrical field
SEM	Scanning electron microscopy
SIMS	Secondary ions mass spectroscopy
TEM	Transmission electron microscopy
XRD	X-ray diffractometer

© COPYRIGHT UPM

LIST OF SYMBOLS

α	Nonlinear coefficient
ε_o	Dielectric constant
θ (^{o})	Diffraction angle
λ (nm)	X-ray wavelength
v_{th} (m/s)	Thermal velocity
ρ_{avg} (g/cm^3)	Average density of ceramic
ρ_{water} (g/cm^3)	Density of water
ρ_{rel} (%)	Average relative density
$\rho_{theoretical}$ (g/cm^3)	Theoretical density
σ_n (cm^2)	Capture cross-sections
ω (m)	Depletion width
ϕ_B (eV)	Potential barrier height
ΔC (pF)	Capacitance transient
ΔT (^{o}C)	Temperature interval
ΔE_T (eV)	Activation energy
%$\Delta\alpha$ (%)	Percent variation in nonlinear coefficient
%ΔE_b (%)	Percent variation in breakdown field
%ΔJ_L (%)	Percent variation in leakage current density
A (A/cm^{2}K^2)	Richardson's constant
A (mm)	Area of metal contact parallel to the edge of the depletion region in semiconductor
c_n (s^{-1})	Electron capture
C_R (pF)	Capacitance value at reverse bias
d (μm)	Average grain size
d-spacing (Å)	Dimension spacing
e_n (s^{-1})	Emission rate
E (V/mm)	Electrical field
E_b (V/mm)	Breakdown field
Ec (eV)	Energy level for the conduction band
E_C-E_T (eV)	Position of trap energy level from the conduction band
E_F (eV)	Fermi energy level
E_V (eV)	Energy level for the valence band
f (Hz)	Lock-in frequency
I (A)	Current
I_L (A)	The total current across varistor ceramic
I_{L1} (A)	Current passing through the DSB at grain boundaries
I_{L2} (A)	Current passing through temperature independent pathways
J (mA/cm^2)	Current density
J_L (μA/cm^2)	Leakage current density
k_B (eV/K)	Boltzmann's constant
L (μm)	Length of a random line drawn on a micrograph of polished sample surface

© COPYRIGHT UPM

k_L ($^oC^{-1}$)	Temperature-dependent coefficient
K_T ($\mu A/min^{1/2}$)	Degradation rate coefficient
M	Magnification of the micrograph
m_{air} (g)	Mass of varistor ceramic pellet in air
m_{water} (g)	Mass of varistor ceramic pellet when submerged in water
m_e	Electron effective mass
N	Number of grain boundaries intercepted by line
N_c (cm^{-3})	Density of state for conduction band
N_d (cm^{-3})	Doping concentration
N_T (cm^{-3})	Concentration of trap
O_{ad}	Adsorbed oxygen
O_i	Interstitial oxygen
P (Watt)	DC power dissipation
r_c (^oC/min)	Cooling ramp
r_h (^oC/min)	Heating ramp
T (K)	Absolute temperature
T_i (^oC)	Initial temperature
T_m (^oC)	Melting temperature
T_{max} (K)	Peak temperature of DLTS signal
T_s (^oC)	Sintering temperature
$t^{1/2}$ ($min^{1/2}$)	Stressing time
t_s (h)	Sintering time
t_f (s)	Pulse filling time
V (V)	Applied DC voltage
V_{1mA} (V)	Breakdown voltage
V_{bi} (V)	Built-in voltage
V_{gb} (V)	Voltage per grain boundary
V_O	Oxygen vacancy
V_{Zn}	Zinc vacancy
V_R (V)	Voltage at reverse biased condition
V_1 (V)	Filling pulse
x	Mol percentage of dopant
Zn_i	Interstitial zinc

© COPYRIGHT UPM

CHAPTER 1

INTRODUCTION

1.0 Introduction

This chapter introduces an overview of nonlinear ZnO varistor for overvoltage protection and an update on the current progress of varistor ceramic development. The problem statements which are the foundation and focus for this study have been highlighted in this chapter. They general raise concerns over varistor degradation phenomena that have posed a great challenge on the production of durable and high performance varistor materials. The significance and contribution of this study towards a better understanding of varistor degradation effects and its mechanism are highlighted. In addition, the research objectives and scopes are defined. In the final part, the organization of thesis is described.

1.1 Research Background

1.1.1 Overview of Metal Oxide Varistor Development

Varistor is a voltage-dependent resistor that demonstrates significant nonlinear current-voltage behaviour. It is incorporated in various electrical protection devices for filtering damaging transient voltage from the load. The transient voltage commonly refers to the voltage surge that exceeds 10% of circuit's operating voltage. Frequent transient voltage that is raised beyond the design voltage limit will stress or breakdown the insulation system and eventually cause damage to an equipment or a circuit. In practice, a varistor is connected in parallel to the protected circuit. Figure 1.1 shows a circuit protected with varistor.

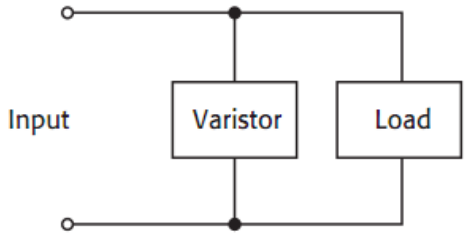

Figure 1.1. Typical placement of varistor in a circuit

Within the normal operating voltage, a varistor remains under high resistance mode (approximately 10^{10} Ω.cm) and appears in open circuit (Eda, 1989). In the event of overvoltage, it will instantaneously change to low resistance state allowing conduction

© COPYRIGHT UPM

of large current resulted from the excess voltage. Energy generated by the transient is also effectively absorbed. Eventually, the destructive voltage is bypassed from the circuit and grounded.

Demands for metal oxide varistors are growing every year and these are driven by ongoing development of both Electrostatic Discharge (ESD) and overvoltage protection devices. The ESD protection requirement for digital electronic circuits in various telecommunication devices and portable electronics has created large market segment for varistors. In addition, the application of varistor as voltage transient protection in automobile electronics and household appliances significantly encourages the global production of varistors. In high voltage applications, overvoltage protection is required for preventing temporary transient voltage, power switching and induced-lightning surges from affecting the distribution or transmission power lines (He and Hu, 2007). In the near future, the movement to smart grids and integration of renewable energy systems will bring a greater positive impact on the use of varistors in circuit protection equipment.

1.1.2 Zinc Oxide Varistors

Most of commercially available varistors are made of solid-state ceramics comprising zinc oxide (ZnO) doped with traces amount of specific metal oxide additives. ZnO is an *n*-type semiconducting material with a large energy band–gap (3.44 eV) (Mishra and Singh, 2007). It offers many good features as key varistor component such as high density and high energy handling capability (Einzinger, 1987). Depending on its power ratings, a ZnO varistor can absorbed between 200 - 250 J/cm^3 of surge-energy and dissipate the heat uniformly across its surface (Wang et al., 2007b). Doping of ZnO with specific additives is crucial to increase the functionality of varistor. The dopants could serve as grain boundary activators (Bi_2O_3, Pr_6O_{11}, SrO, BaO), nonlinearity enhancers (MnO_2, Co_3O_4, Cr_2O_3) and stabilizers (Ag, Sb, B). These additives whether dissolve into the interior of ZnO grains or segregate to create highly insulating intergranular layer in between ZnO grains.

Typical construction of a ZnO varistor device is illustrated in Figure 1.2. It contains highly conductive grains of ZnO core material and three-dimensional network of grain boundaries connected in series or in parallel. Two silver electrode layers covering both upper and lower surfaces of the bulk ZnO ceramic disc allow effective penetration of current across the device during operation. Wire leads are soldered on both electrodes to provide electrical connection. The ceramic is encapsulated with insulating materials such as porcelain or polymeric materials including cured and non-flammable ochre epoxy lacqueur to shield the component from excessive exposure to heat, moisture or oxidative environment.

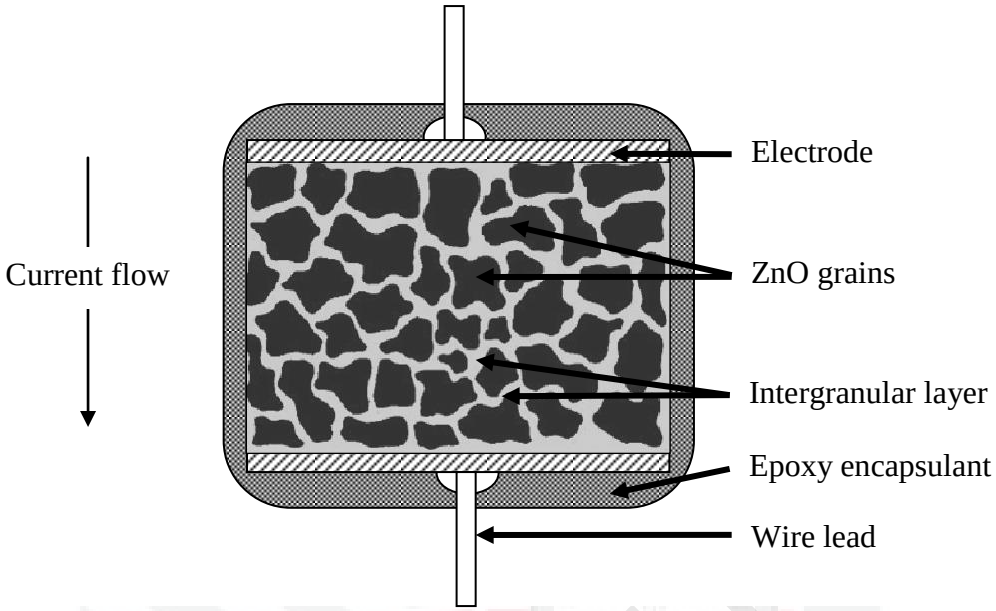

Figure 1.2. A typical construction of a ZnO varistor device

ZnO varistor ceramics are mass-produced through solid- state route technique. This conventional technology involves several important steps such as ball milling, cold pressing and sintering. Powder mixture of ZnO and metal oxide additives of predetermined composition is ball-milled to produce homogenous slurry solution. The slurry is then dehydrated and cold-pressed into compact green body. A heat treatment known as sintering process is performed to transform the compact green body into ceramic of various shape, size and configurations. The sintering process allows solid-state reaction to occur and induces segregation or diffusion of varistor components. Through this array of procedures, the crucial microstructure profile of a varistor could be developed and tailored. Despite its simplicity, high purity and homogeneity sample could hardly be achieved without accurate ball milling settings. Furthermore, high sintering temperature (> 1000 ^{o}C) and longer sintering time are required to obtain uniform and dense-grained varistors. Adversely, such high sintering temperature and prolonged heat treatment cause severe loss of some low volatility and reactive dopants.

In recent years, modified chemical routes provide alternatives for obtaining higher quality, purity and homogeneity ceramic materials. Previous researches highlighted a number of chemical methods suitable for preparing ZnO and other metal oxides such as emulsion precipitation, hydrothermal synthesis, sol-gel, citrate gel (Pechini) and low temperature combustion synthesis. Interestingly, most of these chemical routes producing metal oxide in the form of nanoparticle intermediates. Purity and homogeneity of samples particularly that comprise multicomponent oxides can be controlled during processing.

1.1.3 Electrical Nonlinearity

The competence of ZnO varistors depends on its unique current density, J - electrical field, E characteristics. Figure 1.3 depicts a typical wide-range J-E characteristic of a ZnO varistor. The J-E response of a ZnO varistor can be divided into three distinctive regions which are the pre-breakdown, breakdown and upturn regions.

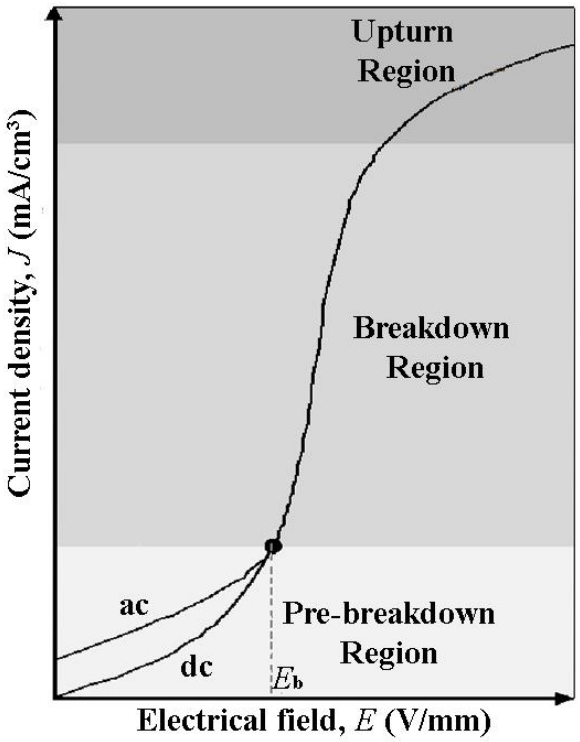

Figure 1.3. Typical J-E characteristic of a ZnO varistor (Adapted from (Gupta, 1990)

i) Pre-breakdown region

Prebreakdown region is known as the Ohmic region. It is the region where a varistor material behaves like an insulator. Below the breakdown field, E_b point, the material will exhibit a linear conduction of current with increasing electrical field. An ideal varistor must remain in high resistive state and permits only small amount of leakage current to pass through it. Within the region, its electrical properties are thermally dependent and determined by the impedance of grain boundaries of ZnO microstructure (Eda, 1989). Electrical conduction is predominantly caused by thermal excitation of electron over potential barriers (Philipp and Levinson, 1979).

ii) Breakdown region

The intermediate region is termed as the breakdown or nonlinear region. The resistance of varistor drastically decreases once the applied electrical field exceeding the E_b point and the signature nonlinear J-E response ($J \propto E^{\alpha}$) will be observed. The varistor material conducts large amount of current for a small increase of electrical field. The J-E characteristics in this region are practically independent of temperature. Conduction mechanism is primarily controlled by tunneling process which involves transportation of electrons through the barriers (Mukae et al., 1977).

iii) Upturn region

The upturn region starts at high current state. The J-E characteristics of this region are similar to those of in pre-breakdown region. The electrical field rising is faster with current compared in the nonlinear region. Within this region, the impedance of the grains in the ZnO microstructure controls the electrical properties of varistor material (Philipp and Levinson, 1979; Gupta, 1990).

The quality of a varistor material is assessed according to several key J-E characteristic parameters. These parameters are the operating voltage, nonlinear coefficient, breakdown field and leakage current. Operating voltage is the range of voltage that could be withstand by the varistor material without damage. The range of operating voltage for low voltage application is 3 – 200 V and a current of 0.1 mA to 1 A. Meanwhile, the operating voltage of high voltage varistor could reach up to 20 kV.

Nonlinear coefficient, α designates the degree of nonlinear electrical response. The exponential relationship between J and E in nonlinear region can be expressed by,

$$J=CE^{\alpha} \tag{1.1}$$

where C is a constant. A greater α value indicates a better varistor. Advancement in ceramic technology has enabled the production of metal oxide varistors having α values of up to 100. As shown in Figure 1.4, the value of α gradually change with J and the relationship has been investigated in (Philipp and Levinson, 1979). Therefore, the range of J where the α value is determined should be clearly stated. The common ranges of J used for extracting the α value are 0.1 to 1 mA/cm^2, 1 to 10 mA/cm^2 and 10 to 100 mA/cm^2. The α value is greatly influenced by composition of varistor ceramic and its sintering conditions.

© COPYRIGHT UPM

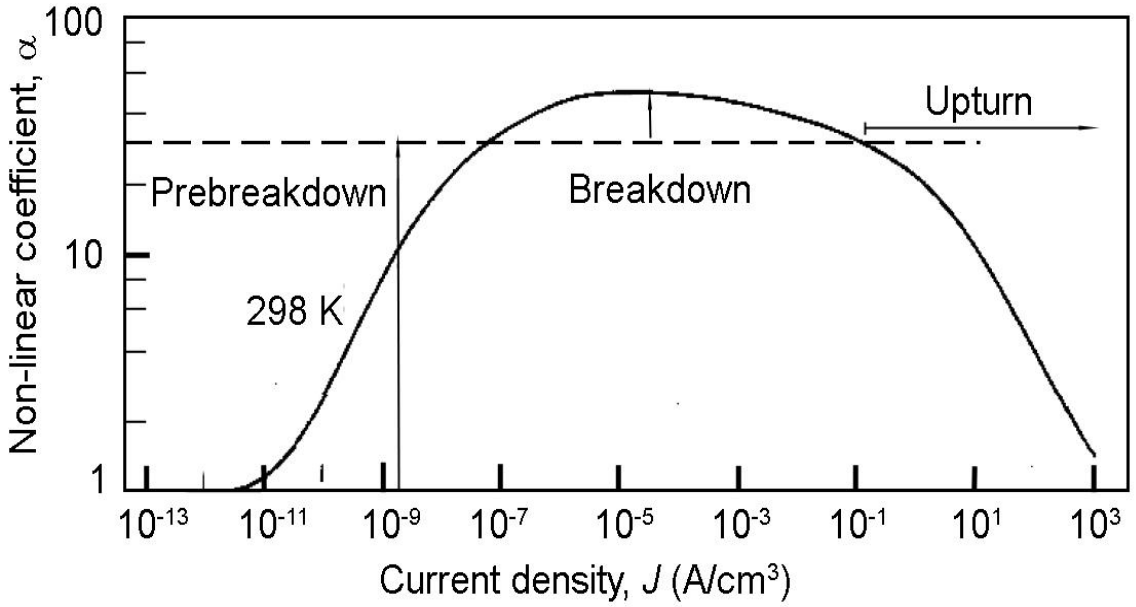

Figure 1.4. Variation in nonlinear coefficient with current density (Adapted from (Philipp and Levinson, 1979))

Breakdown field, E_b is a reference point to mark a transition from linear into nonlinear behavior (Gupta, 1990; Nahm, 2009). Some works use the term breakdown voltage, nominal voltage, switching voltage or varistor voltage to signify the same parameter. It is widely accepted that the value of E_b is defined as the value of electrical field when 1.0 mA/cm^2 of current surge into the varistor material. The E_b value is strongly related to the ZnO grain size and the thickness of the ceramics.

Leakage current density, J_L is the current density when the applied electrical field reach the level of 20% below the E_b point. It indirectly signifies the amount of power dissipation that will be generated during the steady state application of an operating voltage. The higher the leakage current density means the higher the power will be dissipated.

1.1.4 Low-voltage Varistors

Applications of low-voltage ZnO varistors for circuit protection are increasingly significant due to growing demands on low-voltage electronics. For instance, battery powered and mobile appliances require protection from transient voltage of between 4 to 20 V (DC voltage) while many communication devices need fast response protection from transient voltage of 22 to 68 V (Levinson and Philipp, 1986; Gupta, 1990; Pan et al., 2010). Automotive electronics on the other hand requires protection from transient voltage between 16 to 85 V or higher. These factors create needs for continuous development of ZnO varistor materials with low breakdown voltage.

© COPYRIGHT UPM

Fabricating low-voltage ZnO varistors is always demanding. Trade-offs between breakdown voltage and grain size in conventional Bi_2O_3 based ZnO ceramics poses a critical bottle-neck in existing manufacturing of low-voltage varistors. This is because the effective breakdown voltage of a varistor is proportionate to the number of grain boundaries per unit thickness and the inverse to grain size. Consequently, lowering the breakdown voltage in Bi_2O_3-ZnO varistor having average breakdown voltage per individual grain boundary, V_{gb}, of approximately 3.2–3.5 V is a great challenge (Tao et al., 1987; Olsson and Dunlop, 1989; Clarke, 1999).

Most existing preparation techniques rely strongly on ZnO grain manipulation processes. The most classical ways of making low-voltage varistors are through grain coarsening techniques by making varistor from crushed ceramics, prolonged sintering processes at higher temperatures and adding grain growth enhancers such as TiO_2 (Toplan and Karakas, 2002). Other ways include employment of seeding technique by using grown ZnO crystal seeds as precursor (Eda et al., 1983; Hennings et al., 1990; Souza et al., 2003) and deposition technique to fabricate multilayered thin film varistor ceramics with interdigitated electrodes (Kuo et al., 2008). Grain coarsening and seeding techniques could be economically less feasible as they are energy intensive processes and the resultant ceramics suffer from inhomogeneous microstructure which leads to inconsistent current-voltage characteristics (Hennings et al., 1990). Multilayered thin film varistors obtained from deposition technique on the other hand, are lingered with structural integrity issues (Kuo et al., 2008). Constraints in many preparation techniques of low-voltage ZnO varistors suggest the need for more reliable options.

Employment of modified chemical approach into fabrication of low-voltage varistor ceramics may potentially overcome some of present limitations. There have been a number of valuable studies reporting the successful preparation of ZnO varistors through wet chemical techniques including sol-gel, co-precipitation, citrate and hydrothermal methods (Hohenberger and Tomandl, 1992; Lorenz et al., 2001a; Lorenz et al., 2001b; Durán et al., 2002; Ribeiro et al., 2005; Yang et al., 2005; Li et al., 2006; Lupan et al., 2008; Sun et al., 2012). The chemical approach offers many key advantages over solid-state route including higher compositional homogeneity, lower sintering temperature requirement and microstructure homogeneity (Lorenz et al., 2001a; Durán et al., 2002; Dhage et al., 2003; Fan et al., 2009). Conversely, these efforts mostly concert towards high voltage applications and very few attempts have been made so far to adopt the technique in low-voltage varistor ceramic fabrication. Therefore, it is significant to extend the study on development of low-voltage varistor ceramics through employment of modified chemical techniques.

© COPYRIGHT UPM

1.1.5 Praseodymium Oxide Based ZnO Varistors

Research trend shows that Pr_6O_{11} based ZnO ceramics have been actively researched to overcome drawbacks in conventional Bi_2O_3 based ZnO varistor materials such as Bi_2O_3 vaporization and formation of Bi-containing secondary phases when sintered at temperatures over 1000 °C (Cordaro et al., 1986; Simpson and Cordaro, 1990; Winston and Cordaro, 1990; Wang et al., 1996; Nahm, 2003). Ramirez et al., (2008b) and Furtado et al., (2005) demonstrated that Pr_6O_{11} improved effective electrical current flow by restraining the formation of secondary phases and induced densification of varistor during fabrication. Zhu et al., (2008) claimed that Pr_6O_{11} exhibited grain growth suppressing effect that controlled the overall development of grain during sintering. Thus, their studied varistor ceramics had more uniform and compact microstructures. Several series of high density and high stability Pr_6O_{11} based ZnO varistor ceramic systems containing more than four combination of rare earth and transition metal oxides have been developed and reported in Nahm (2003; 2009). The proposed varistor formulations exhibited comparable nonlinear properties to those of Bi_2O_3 based ZnO varistor ceramics with minimum number of additives. The nonlinear coefficient of these ceramics could reach up to 60 with the general V_{gb} of 2-3 V. However, most of Pr_6O_{11} based ZnO varistor systems that have been reported so far are developed for high-voltage applications. The work by Horio et al., (1998) is one of the very few attempts to extend the use of Pr_6O_{11} based ZnO ceramics for low-voltage applications. They have successfully fabricated ZnO/Pr_6O_{11} multilayered thin films having the α value of 10 and E_b value of 20 V by the radio-frequency sputtering in Ar/O_2 environment. Hence, further research is needed in order to take advantage of these potentially high nonlinearity and high stability ceramic materials for satisfying low-voltage requirements.

1.1.6 Varistor Degradation

Performance stability is a major concern in the fabrication of commercial ZnO varistors. This is to ensure their robustness to operate under vigorous conditions for long term applications. Varistors to be used in automobile electronics for instance, should perform their intended functions consistently with low failure rates within the operating temperature between -55 to 125 ^oC for more than 1000 cycles. They are subjected to a variety of disturbances like lightning strikes, switching transients, continuous or temporary overvoltages. Upon application of stress, the variation in breakdown voltage must not exceed more that 10%. In fact, many international standards such as Automotive Electronic Council – Q200 even enforce more stringent quality assurance guideline for the use of varistor in automotive parts to guarantee the reliability of system operation and users' safety.

Degradation phenomena observed in many ZnO based varistor ceramics possibly impede the long-term viable application of the device. Varistor performance degrades under application of single or combination of stresses including high temperature, repetitive or continous electrical stress, humidity and reducing atmosphere. Degradation effects manifest itself as a decline in α and E_b values which accompanied with a drastic

© COPYRIGHT UPM

increment in J_L with time. These signs indicate a significant disappearance of nonlinearity and shifting of properties towards Ohmic behaviour. To certain extent, a degraded varistor could experience thermal runaway resulting in overheating or potentially explosion. Some of degraded varistors become asymmetrical in polarity and exhibit increment in terms of its capacitance component (Einzinger, 1987; Jaroszewski et al., 2004).

In recent years, the study of degradation in ZnO varistor ceramics have been focused on several aspects such as the evaluation of varistor response under various forms and intensity of stresses, determination of degradation effects on electrical and chemical properties of varistor ceramics and the modelling of electronic and chemical mechanisms that drive degradation process of ZnO varistor ceramics.

1.2 Problem Statements

Degradation phenomena in commercial and lab-synthesized ZnO varistor ceramics under diverse forms of stress conditions have been investigated since the early 1980's (Sonder et al., 1985; Zhou et al., 2003; Wang et al., 2007a; Nahm, 2008a, 2012). The ultimate motivation for these efforts is to realize the production of high performance and high stability varistor materials. Despite extensive research reports on conventional high-voltage Bi_2O_3 type varistor ceramics, very little attention has been paid on investigating the degradation phenomena in low-voltage ceramics (Clarke, 1999).

Pr_6O_{11} based ZnO ceramics with many promising properties are continuously formulated and characterized for new generation ZnO varistors. Meanwhile, the interest to adopt nano-fabrication and chemical approaches in varistor fabrication process is now growing. Although comprehensive property characterizations have been performed on several series of ceramics, the degradation behaviour of low-voltage Pr_6O_{11} based ZnO varistor ceramics against electrical and temperature stresses remain unclear. Within the years 1999 to 2012, Nahm and co-workers have comprehensively studied the degradation behaviour of several high voltage Pr_6O_{11} based ZnO varistor ceramics derived through solid state routes. To the author's knowledge, there are in fact, no degradation study have been carried out on low-voltage Pr_6O_{11} based ZnO varistors derived by chemical techniques.

Degradation mechanisms in ZnO varistor is still an area of long-standing confusion and debate. Ongoing advancement in varistor processing continuously increases the complexity in varistor compositions and microstructure. Due to these reasons, the dominant mechanisms that take place during degrading process are always in dispute. It is expected that new insights into degradation mechanisms of varistor ceramics could be provided by observing the direct changes of electronic states at interface level as a result of degradation. The idea can be realized through utilization of deep level transient spectroscopy (DLTS) technique. Lang (1974) demonstrated that quantification of deep

© COPYRIGHT UPM

traps or energy levels in barrier depletion region of semiconductors is made possible by using DLTS. Since then, several works have been performed to identify deep level parameters of ZnO varistors and their relationship to processing methods, compositions and electrical characteristics (Orlandi et al., 2004; Fan and Freer, 2007; Bueno et al., 2008). Unfortunately, detailed DLTS study to compare the deep level characteristics prior to and after degradation test specifically for Pr_6O_{11} based ZnO varistors has never been presented so far. Consequently, mechanisms driving degradation in that specific varistor system could not be satisfactorily understood.

In this study, ZnO varistor ceramics with low breakdown voltage were prepared through employment of a wet chemical approach known as modified citrate gelation method. Four ceramic systems were prepared by doping ZnO with single Pr_6O_{11} dopant and/or added with transition metal oxide additives (Co, Mn, Cr). Variations in microstructure and nonlinear electrical characteristics of the prepared ceramics as a function of dopant contents and sintering conditions were determined and discussed. The degradation behaviour of these varistors against DC electrical field and high temperature stresses was thoroughly investigated. The degradation process in Pr_6O_{11} based ZnO varistors were also discussed on the basis of DLTS analysis.

1.3 Research Objectives

The primary aim of this study was to investigate the degradation phenomena of Pr_6O_{11} based ZnO varistor ceramics which were obtained through modified citrate gelation method. To achieve the goal, the following four research objectives have been formulated.

i) To study effects of dopant contents on microstructure and nonlinear electrical characteristics of Pr_6O_{11} based ZnO varistor ceramics prepared through modified citrate gelation technique.
ii) To study effects of sintering conditions (time and temperature) on microstructure and nonlinear electrical characteristics of Pr_6O_{11} based ZnO varistor ceramics prepared through modified citrate gelation technique.
iii) To investigate effects of simultaneous DC electrical field and high temperature stresses on nonlinear electrical characteristics of Pr_6O_{11} based ZnO varistor ceramics.
iv) To investigate the influence of deep levels on degradation behaviour of Pr_6O_{11} based ZnO varistor ceramics using deep level transient spectroscopy technique.

It is hypothesized that the average grain size and relative density of sintered ceramics will increase when the contents of MnO_2 and Co_3O_4 increase whereas they will decrease when the contents of Pr_6O_{11} and Cr_2O_3 increase. These properties will also increase when the sintering time and temperature increase. The nonlinear coefficient, α of the doped ZnO ceramics will increase up to a certain extent of doping contents, sintering temperature or time.

© COPYRIGHT UPM

The nonlinear properties of the ZnO varistor ceramics doped with Pr_6O_{11}, Co_3O_4, MnO_2 and Cr_2O_3 will degrade when exposed to continuous application of DC electrical field at elevating temperature for prolonged duration. Degradation of Pr_6O_{11} based ZnO varistor ceramics will result in a decrease in concentration of bulk traps and the interface traps. Degradation also causes shifting of trap activation energy due to the emergence of new defect clusters near to grain boundary interface.

1.4 Research Scopes

In order to achieve the above-mentioned research objectives, several scopes of works have been drawn. It has been determined that the study of degradation phenomena discussed in this thesis is limited to low-voltage Pr_6O_{11} based ZnO varistor (breakdown field less than 200 V/mm). Four ceramic systems have been developed and the nominal composition of each system is listed;

i) System 1: $(100 - x)$ mol% ZnO + x mol% Pr_6O_{11}
ii) System 2: $(99.2 - x)$ mol% ZnO + 0.8 mol% Pr_6O_{11} + x mol% Co_3O_4
iii) System 3: $(99.2 - x)$ mol% ZnO + 0.8 mol% Pr_6O_{11} + x mol% MnO_2
iv) System 4: $(99.2 - x)$ mol% ZnO + 0.8 mol% Pr_6O_{11} + x mol% Cr_2O_3

(where x = 0, 0.2, 0.4, 0.6, 0.8, 1.0)

All ceramic systems have been prepared only through employment of modified citrate gelation technique and solid-state sintering. The content for dopant of interest was varied between 0.2 to 1.0 mol%. The sintering temperatures applied were 1200, 1225, 1250 and 1275 ^oC and the sintering time applied were 1, 3, 5 and 7 h.

All ceramic systems were characterized in terms of their microstructure and electrical properties. Microstructure analysis was performed by X-ray diffraction, Field emission scanning electron microscopy and energy dispersive X-ray spectroscopic techniques. Electrical analysis was conducted on the basis of J-E characteristic measurement at 30 ^oC using source-measure unit that supplies a maximum DC voltage of 100 V and measures current up to 100 mA. A varistor ceramic with optimized dopant content from each system was sent for DC degradation test. The stress conditions applied in sequence were ($0.85E_b$/30 ^oC/ / 18 h), ($0.85\ E_b$/ 60 ^oC/18 h) and ($0.85E_b$/125 ^oC/18 h). Deep level characterization prior to and after the DC degradation test was performed using deep level transient spectroscopy (DLTS) technique. Deep level parameters such as trap concentration, N_T, trap activation energy, E_T and capture cross section, σ_n, were extracted from DLTS spectra collected from temperature scanning mode in the range of 100 to 440 K.

1.5 Research Significance

The study of degradation phenomena in Pr_6O_{11} based ZnO varistor ceramics can provide more scientific evidences on the robustness of low-voltage Pr_6O_{11} based ZnO varistor ceramics against electrical and high temperature degradation. This is relevance since many existing studies highlighted the vulnerability low-voltage system to degradation. This is because the system generally exhibits relatively low α and susceptibility to "hot spots" due to non-uniform grain size distributions (Han et al., 1995; Suzuki and Bradt, 1995; Wang et al., 2008).

The findings from this study can be useful in clarifying the role of Pr_6O_{11}, the transition metal oxide additives particularly the oxides of Co, Mn and Cr as well as their synergistic effects on stability of ZnO varistor. Therefore, the information is valuable in optimizing the varistor performance through appropriate selections of varistor's components.

The findings from this study can be a reference for future development of ZnO varistor ceramics prepared through nano-fabrication and chemical approaches which is currently lacking. The preparation of varistor ceramics through the modified citrate gelation method, outlined in this study can be potentially optimized for more complex formulation and scaling up. Additionally, the outcome of this study can be use as basis for assessing the reliability of varistor products obtained through chemical processes.

The study of degradation process in Pr_6O_{11} based ZnO varistor ceramic by means of DLTS can provide more explanation on the relationship between deep level characteristics of ZnO and DC degradation process. The contribution of intrinsic defects of ZnO and impurities towards the stability against DC electrical field and high temperature stresses for prolonged duration can be further justified. This contribution is valuable towards development of Pr_6O_{11} based ZnO varistor ceramics with improved stability and durability in the near future.

1.6 Thesis Organization

The thesis is organized into six main chapters. Chapter 1 presents the preface to the thesis. It covers the summary of research background, issues and key challenges facing ZnO varistor development. The research objectives and scopes are also described. Chapter 2 comprises a review on development of ZnO nonlinear varistor ceramics. It covers the historical evolution of nonlinear varistor materials, development of ZnO varistor microstructure and the analysis on roles of various varistor dopants reported in previous studies. Detailed aspects of varistor degradation phenomena and substantive findings from studies of varistor degradation using deep level transient spectroscopy technique are thoroughly reviewed. Chapter 3 gives detailed description on ZnO intrinsic properties, theoretical models related to conduction mechanisms and

© COPYRIGHT UPM

degradation phenomena in ZnO varistor ceramics. The theory of deep levels and principles of DLTS measurement are elaborated. Chapter 4 outlines the synthesis process to obtain four series of Pr_6O_{11} based ZnO ceramic systems according to modified citrate gelation approach and solid-state sintering. The implementation of the process and issues encountered during the preparation are described. In addition, the chapter also provides explanation on every characterization method performed to analyze both electrical and microstructure properties of produced ceramics. Chapter 5 is divided into four divisions to present the results and discussion on four Pr_6O_{11} based ZnO ceramic systems. In each division, the related findings and observation collected from both microstructure and electrical studies are presented. Effects of dopant contents and sintering conditions on nonlinear electrical properties of Pr_6O_{11} based ZnO varistor ceramics are described and correlated to variation in microstructure or electrical behaviour. DC degradation characteristics and its effects on nonlinear electrical properties are also clarified. In addition, the influence of deep levels on nonlinear electrical properties and its linkage to DC degradation phenomena are conferred. Chapter 6 concludes the general outcomes from arguments presented in preceding chapters. For future works, limitations on current studies and recommendations for future research are highlighted.

© COPYRIGHT UPM

REFERENCES

Al-Abdullah, K. (2012). Elaboration of ZnO based varistors and the effect of the rare-earths on their electrical behaviour. *Energy Procedia. 19*: 116-127.

Alles, A. B. and Burdick, V. L. (1991). The effect of liquid phase sintering on the properties of Pr_6O_{11} based ZnO varistors. *Journal of Applied Physics. 70*(11): 6883-6890.

Alves, M. C. F., Souza, S. C., Lima, S. J. G., Longo, E., Souza, A. G. and Santos, I. M. G. (2007). Influence of the precursor salts in the synthesis of $CaSnO_3$ by the poymeric precursor method. *Journal of Thermal Analysis and Calorimetry. 87*(3): 763-766.

Ammar, A. H. and Farag, A. A. M. (2010). Investigation of deep level transient spectroscopy (DLTS) of dopant ZnO-based varistors. *Physica B: Physics of Condensed Matter. 405*(6): 1518-1522.

Ananthakumar, S., Anas, S., Ambily, J. and Mangalaraj, R. (2010). Microwave assisted citrate gel combustion synthesis of ZnO Part-I: Assessment of structural features. *Journal of Ceramic Processing Research. 11*(1): 29-34.

Ananthakumar, S., Varma, H. K., Perumal, P., Rao, P. P., Damodaran, A. D. and Warrier, K. G. K. (1994). Effect of addition of calcined grains on the microstructure and non-linearity features of ZnO varistors. *Journal of Materials Science Letters. 13*(10): 731-733.

Anas, S., Mukundan, P., Sanoj, A. M., Mangalaraja, V. R. and Ananthakumar, S. (2010). Synthesis of ZnO based nanopowders via non-hydrolytic sol-gel technique and their densification behaviour and varistor properties. *Processing and Application of Ceramic. 4*(1): 7-14.

Arrillaga, J. (1998). *High voltage direct current transmission* (2nd ed.). London: The Institute Engineering and Technology.

Asokan, T. and Freer, R. (1994). Dependence of ZnO varistor grain boundary resistance on sintering temperature. *Journal of Materials Science Letters. 13*(13): 925-926.

© COPYRIGHT UPM

Baptista, J. L. and Mantas, P. Q. (2000). High temperature characterization of electrical barriers in ZnO varistors. *Journal of Electroceramics. 4*(1): 215-224.

Bernik, S., Zupančič, P. and Kolar, D. (1999). Influence of Bi_2O_3/TiO_2, Sb_2O_3 and Cr_2O_3 doping on low-voltage varistor ceramics. *Journal of the European Ceramic Society. 19*(6–7): 709-713.

Bueno, P. R., Leite, E. R., Oliveira, M. M., Orlandi, M. O. and Longo, E. (2001). Role of oxygen at the grain boundary of metal oxide varistors: A potential barrier formation mechanism. *Applied Physics Letters. 79*(1): 48-50.

Bueno, P. R., Varela, J. A. and Longo, E. (2008). SnO_2, ZnO and related polycrystalline compound semiconductors: An overview and review on the voltage-dependent resistance (non-ohmic) feature. *Journal of the European Ceramic Society. 28*(3): 505-529.

Carlsson, J. M., Domingos, H. S., Bristowe, P. D. and Hellsing, B. (2003). An interfacial complex in ZnO and its influence on charge transport. *Physical Review Letters. 91*(16): 165506.

Castro, M. S. and Aldao, C. M. (1996). Different degradation processes in ZnO varistors. *Ceramics International. 22*(1): 39-43.

Chen, H.-L., Lin, C.-C., Lee, W.-S. and Whu, W.-H. (2008). A study on the relationship between material and electrical properties of ZnO-based varistors. *Journal of the Chinese Institute of Engineers. 31*(2): 343-347.

Chen, W. and Chan, H. L. W. (2004). Degradation of ZnO ceramic varistors induced by water and AC voltages. *Japanesse Journal of Applied Physics. 43*(2): 701-702.

Cheng, L., Li, G., Yuan, K., Meng, L. and Zheng, L. (2012). Improvement in nonlinear properties and electrical stability of ZnO varistors with B_2O_3 additives by nano-coating method. *Journal of the American Ceramic Society. 95*(3): 1004-1010.

Chiang, Y. M., Kingery, W. D. and Levinson, L. M. (1982). Compositional changes adjacent to grain boundaries during electrical degradation of a ZnO varistor. *Journal Applied Physics. 53*(2): 1765-1769.

© COPYRIGHT UPM

Chun, S.-Y. and Mizutani, N. (2001). Mass transport via grain boundary in Pr-based ZnO varistors and related electrical effects. *Materials Science and Engineering: B. 79*(1): 1-5.

Chun, S.-Y., Wakiya, N., Funakubo, H., Shinozaki, K. and Mizutani, N. (1997). Phase diagram and microstructure in the ZnO–Pr_2O_3 System. *Journal of the American Ceramic Society. 80*(4): 995-998.

Clarke, D. R. (1978). The microstructural location of the intergranular metal-oxide phase in a zinc oxide varistor. *Journal Applied Physics. 49*(4): 2407-2411.

Clarke, D. R. (1999). Varistor ceramics. *Journal of American Ceramic Society. 82*(3): 485-502.

Cordaro, J. F., Shim, Y. and May, J. E. (1986). Bulk electron traps in zinc oxide varistors. *Journal of Applied Physics. 60*(12): 4186-4190.

Dhage, S. R., Pasricha, R. and Ravi, V. (2003). Synthesis of ultrafine TiO_2 by citrate gel method. *Materials Research Bulletin. 38*(11–12): 1623-1628.

Dillon, S. J., Behera, S. K. and Harmer, M. P. (2008). An experimentally quantifiable solute drag factor. *Acta Materialia. 56*(6): 1374-1379.

Domingos, H. S., Carlsson, J. M., Bristowe, P. D. and Hellsing, B. (2004). The formation of defect complexes in a ZnO grain boundary. *Interface Science. 12*(2-3): 227-234.

Duan, L. B., Zhao, X. R., Liu, J. M., Wang, T. and Rao, G. H. (2010). Room-temperature ferromagnetism in lightly Cr-doped ZnO nanoparticles. *Applied Physics A. 99*(3): 679-683.

Durán, P., Capel, F., Tartaj, J. and Moure, C. (2002). Low-temperature fully dense and electrical properties of doped-ZnO varistors by a polymerized complex method. *Journal of the European Ceramic Society. 22*(1): 67-77.

Ebrahimizadeh Abrishami, M., Kompany, A. and Hosseini, S. M. (2012). Varistor behavior of Mn doped ZnO ceramics prepared from nanosized precursors. *Journal of Electroceramics. 29*(2): 125-132.

© COPYRIGHT UPM

Eda, K. (1978). Conduction mechanism of non-Ohmic zinc oxide ceramics. *Journal of Applied Physics. 49*(5): 2964-2972.

Eda, K. (1989). Zinc oxide varistor. *IEEE Electrical Insulation Magazine. 5*(6): 28-41.

Eda, K., Iga, A. and Matsuoka, M. (1980). Degradation mechanism of non-Ohmic zinc oxide ceramics. *Journal of Applied Physics. 51*(5): 2678-2684.

Eda, K., Inada, M. and Matsuoka, M. (1983). Grain growth control in ZnO varistors using seed grains. *Journal Applied Physics. 54*(2): 1095-1099.

Egashira, M., Shimizu, Y., Takao, Y. and Fukuyama, Y. (1996). Hydrogen-sensitive breakdown voltage in the I–V characteristics of tin dioxide-based semiconductors. *Sensors and Actuators B: Chemical. 33*(1–3): 89-95.

Einzinger, R. (1982). Grain boundary phenomena in ZnO varistors. *Journal of Applied Physics D: Applied Physics. 17*(2): 343-355.

Einzinger, R. (1987). Metal oxide varistors. *Annual Review of Materials Science 17*: 299-321.

Erhart, P. and Albe, K. (2006). Diffusion of zinc vacancies and interstitials in zinc oxide. *Applied Physics Letters. 88*(20): 201981 - 201983.

Ezhilvalavan, S. and Kutty, T. R. N. (1996). Dependence of non-linearity coefficients on transition metal oxide concentration in simplified compositions of $ZnO+Bi_2O_3+MO$ varistor ceramics (M=Co or Mn). *Journal of Materials Science: Materials in Electronics. 7*(2): 137-148.

Fan, J. and Freer, R. (1993). The electrical properties and d.c. degradation characteristics of silver doped ZnO varistors. *Journal of Materials Science. 28*(5): 1391-1395.

Fan, J. and Freer, R. (1994). Deep level transient spectroscopy of zinc oxide varistors doped with aluminum oxide and/or silver oxide. *Journal of the American Ceramic Society. 77*(10): 2663-2668.

Fan, J. and Freer, R. (1997). Varistor properties and microstructure of ZnO–BaO ceramics. *Journal of Materials Science. 32*(2): 415-419.

© COPYRIGHT UPM

Fan, J. and Freer, R. (2007). Deep level transient spectroscopy of SnO_2-based varistors. *Applied Physics Letters. 90*(9): 093511.

Fan, J., Zhang, Z., Tian, H., Zhao, H. and Freer, R. (2009). Investigation of the effect of different dopants on the trap states of ZnO-based and SnO_2-based varistors *Journal of Physics: Conference Series 152*(1): 012060.

Fan, J. C., Sreekanth, K. M., Xie, Z., Chang, S. L. and Rao, K. V. (2013). *p*-Type ZnO materials: Theory, growth, properties and devices. *Progress in Materials Science. 58*(6): 874-985.

Ferro, S. (2011). Physicochemical and electrical properties of praseodymium oxides. *International Journal of Electrochemistry. 2011*: 1-7.

Fu, X. L., Zang, Y. X. and Peng, Z. J. (2014). Effect of WO_3 doping on microstructural and electrical properties of ZnO-Pr_6O_{11} based varistor materials. *Key Engineering Materials. 591*: 54-60.

Furtado, J. G. d. M., Saléh, L. A., Serra, E. T., Oliveira, G. S. G. d. and Nóbrega, M. C. d. S. (2005). Microstructural evaluation of rare-earth-zinc oxide-based varistor ceramics. *Materials Research. 8*: 425-429.

García, M. A., Ruiz-González, M. L., Quesada, A., Costa-Krämer, J. L., Fernández, J. F., Khatib, S. J., Wennberg, A., Caballero, A. C., Martín-González, M. S., Villegas, M., Briones, F., González-Calbet, J. M. and Hernando, A. (2005). Interface double-exchange ferromagnetism in the Mn-Zn-O system: New class of biphase magnetism. *Physical Review Letters. 94*(21): 2172061-2172064.

Gillot, B., Guendouzi, M. E. and Laarj, M. (2001). Particle size effects on the oxidation-reduction behavior of Mn_3O_4 hausmannite. *Materials Chemistry and Physics. 70*: 54-60.

Greuter, F. (1995). Electrically active interfaces in ZnO varistors. *Solid State Ionics. 75*(0): 67-78.

Gupta, T. K. (1990). Application of zinc oxide varistors. *Journal of the American Ceramic Society. 73*(7): 1817-1840.

© COPYRIGHT UPM

Gupta, T. K. and Carlson, W. G. (1985). A grain boundary defect model for instability/stability of a ZnO varistor. *Journal of Materials Science. 20*(10): 3487-3500.

Haddad, A. (2004). ZnO surge arrester. In D. F. Warne & A. Haddad (Eds.), *Advances in High Voltage Engineering*. London: The Institution of Engineering and Technology, London, UK.

Han, J.-H., Lee, D.-H. and Kim, D.-Y. (1995). Fabrication of low-voltage ZnO varistors by a two-step process. *Journal of the European Ceramic Society. 15*(4): 371-375.

Han, J., Mantas, P. Q. and Senos, A. M. R. (2002a). Defect chemistry and electrical characteristics of undoped and Mn-doped ZnO. *Journal of the European Ceramic Society. 22*(1): 49-59.

Han, J., Senos, A. M. R. and Mantas, P. Q. (2002b). Deep donors in polycrystalline Mn-doped ZnO. *Materials Chemistry and Physics. 75*(1–3): 117-120.

Hayashi, M., Haba, M., Hirano, S., Okamoto, M. and Watanabe, M. (1982). Degradation mechanism of zinc oxide varistors under dc bias. *Journal Applied Physics. 53*(8): 5754-5763.

He, J. L. and Hu, J. (2007). Discussions on nonuniformity of energy absorption capabilities of ZnO varistors. *IEEE Transactions on Power Delivery. 22*(3): 1523-1532.

He, W., Zhang, Y., Zhang, X., Wang, H. and Yan, H. (2003). Low temperature preparation of nanocrystalline Mn_2O_3 via ethanol-thermal reduction of MnO_2. *Journal of Crystal Growth. 252*(1–3): 285-288.

Hennings, D. F. K., Hartung, R. and Reijnen, P. J. L. (1990). Grain size control in low-voltage varistors. *Journal of the American Ceramic Society. 73*(3): 645-648.

Hng, H. H. and Knowles, K. M. (2002). Microstructure and current-voltage characteristics of praseodymium-doped zinc oxide varistors containing MnO_2, Sb_2O_3 and Co_3O_4. *Journal of Materials Science. 37*(6): 1143-1154.

Hohenberger, G. and Tomandl, G. (1992). Sol-gel processing of varistor powders. *Journal of Materials Research. 7*(3): 546-548.

© COPYRIGHT UPM

Hong, Y. W. and Kim, J. H. (2004). The electrical properties of Mn_3O_4-doped ZnO. *Ceramics International. 30*(7): 1301-1306.

Horio, N., Hiramatsu, M., Nawata, M., Imaeda, K. and Torii, T. (1998). Preparation of zinc oxide/metal oxide multilayered thin films for low-voltage varistors. *Vacuum. 51*(4): 719-722.

Houabes, M. and Metz, R. (2007). Rare earth oxides effects on both the threshold voltage and energy absorption capability of ZnO varistors. *Ceramics International. 33*(7): 1191-1197.

Hu, J., He, J., Long, W. and Liu, J. (2010). Temperature dependences of leakage currents of ZnO varistors doped with rare-earth oxides. *Journal of the American Ceramic Society. 93*(8): 2155-2157.

Ilyas, U., Rawat, R. S., Wang, Y., Tan, T. L., Lee, P., Chen, R., Sun, H. D., Li, F. and Zhang, S. (2012). Alteration of Mn exchange coupling by oxygen interstitials in ZnO:Mn thin films. *Applied Surface Science. 258*(17): 6373-6378.

Inoue, Y., Okamoto, Y. and Morimoto, J. (2008). Thermoelectric properties of porous zinc oxide ceramics doped with praseodymium. *Journal of Materials Science. 43*(1): 368-377.

Jagadish, C. and Pearton, S. J. (2011). *Zinc oxide bulk, thin films and nanostructures: processing, properties, and applications*: Elsevier Science.

Jakani, M., Campet, G., Claverie, J., Fichou, D., Pouliquen, J. and Kossanyi, J. (1985). Photoelectrochemical properties of zinc oxide doped with 3d elements. *Journal of Solid State Chemistry. 56*(3): 269-277.

Janotti, A. and Van de Walle, C. G. (2007). Native point defects in ZnO. *Physical Review B. 76*(16): 1652021-16520222.

Jaroszewski, M., Wieczorek, K., Bretuj, W. and Kostyla, P. (2004). *Capacitance changes in degraded metal oxide varistors.* Paper presented at the Proceedings of the 2004 IEEE International Conference on Solid Dielectrics (ICSD 2004)

Kang, S. J. L. (2005). *Sintering: Densification, grain growth and microstructure*. Oxford, United Kingdom: Elsevier Butterworth-Heinemann.

© COPYRIGHT UPM

Kang, S. J. L., Choi, J. Y., Chang, D. H. and Yoon, Y. S. (2005). A study on the growth and piezoelectric characteristics of ZnO thin film using RF magnetron sputtering method. *Journal of the Korean Physical Society. 47*: S589-S594.

Kang, Z. and Eyring, L. (1998). Fluorite structural principles: Disordered α-phase to ordered intermediate phases in praseodymia. *Journal of Alloys and Compounds. 275*: 721-724.

Kim, J., Kimura, T. and Yamaguchi, T. (1989). Effect of bismuth of oxide content on the sintering of zinc oxide. *Journal of the American Ceramic Society. 72*(8): 1541-1544.

Kuo, S.-T., Tuan, W.-H., Lao, Y.-W., Wen, C.-K., Chen, H.-R. and Lee, H.-Y. (2008). Investigation into the interactions between Bi_2O_3-doped ZnO and AgPd electrode. *Journal of the European Ceramic Society. 28*(13): 2557-2562.

Kutty, T. R. N. and Philip, S. (1995). Low voltage varistors based on $SrTiO_3$ ceramics. *Materials Science and Engineering: B. 33*(2–3): 58-66.

Lang, D. V. (1974). Deep level transient spectroscopy: A new method to characterize traps in semiconductors. *Journal Applied Physics. 45*(7): 3023-3033.

Leach, C., Vernon-Parry, K. and Ali, N. (2010). Deep level transient spectroscopy study of the effect of Mn and Bi doping on trap formation in ZnO. *Journal of Electroceramics. 25*(2-4): 188-197.

Lee, W.-I. and Young, R.-L. (1996). Defects and degradation in ZnO varistor. *Applied Physics Letters. 69*(4): 526-529.

Lee, Y.-S., Liao, K.-S. and Tseng, T.-Y. (1996). Microstructure and crystal phases of praseodymium oxides in zinc oxide varistor ceramics. *Journal of the American Ceramic Society. 79*(9): 2379-2384.

Lei, K., Dongmei, J. and Xueming, M. (2009). Low-temperature sintering of high voltage gradient ZnO-based thick film varistors. *Ceramics-Silikaty. 53*(2): 102-107.

Leite, E. R., Varela, J. A. and Longo, E. (1992). A new interpretation for the degradation phenomenon of ZnO varistors. *Journal of Materials Science. 27*(19): 5325-5329.

© COPYRIGHT UPM

Levinson, L. M. and Philipp, H. R. (1975). The physics of metal oxide varistors. *Journal Applied Physics. 46*(3): 1332-1341.

Levinson, L. M. and Philipp, H. R. (1986). Zinc oxide varistor - A review. *Journal of American Ceramic Society. 65*(4): 639-646.

Li, C., Wang, J., Su, W., Chen, H., Wang, W. and Zhuang, D. (2001). Investigation of electrical properties of $SnO_2{\cdot}Co_2O_3{\cdot}Sb_2O_3$ varistor system. *Physica B: Condensed Matter. 307*(1–4): 1-8.

Li, T. Y., Wang, H. Q., Hua, Z. Q., Dong, L., Zhao, H. W. and Wang, Y. (2010). Densification and grain growth of CuO-doped Pr_6O_{11} varistors. *Ceramics International. 36*(5): 1511-1516.

Li, Y., Li, G. and Yin, Q. (2006). Preparation of ZnO varistors by solution nano-coating technique. *Materials Science and Engineering: B. 130*(1–3): 264-268.

Lin, Y.-H., Cai, J., Li, M., Nan, C.-W. and He, J. (2008). Grain boundary behavior in varistor-capacitor TiO_2-rich $CaCu_3Ti_4O_{12}$ ceramics. *Japanese Journal of Applied Physics. 108*(7): 074111.

Liu, M., Kitai, A. H. and Mascher, P. (1992). Point defects and luminescence centres in zinc oxide and zinc oxide doped with manganese. *Journal of Luminescence. 54*(1): 35-42.

Lorenz, A., Ott, J., Harrer, M., Preissner, E. A., Whitehead, A. H. and Schreiber, M. (2001a). Modified citrate gel routes to ZnO-based varistors. *Journal of the European Ceramic Society. 21*(10–11): 1887-1891.

Lorenz, A., Ott, J., Harrer, M., Preissner, E. A., Whitehead, A. H. and Schreiber, M. (2001b). Modified citrate gel techniques to produce ZnO-based varistors (Part I—Microstructural characterisation). *Journal of Electroceramics. 6*(1): 43-54.

Lupan, O., Shishiyanu, S., Chow, L. and Shishiyanu, T. (2008). Nanostructured zinc oxide gas sensors by successive ionic layer adsorption and reaction method and rapid photothermal processing. *Thin Solid Films. 516*: 3338-3345.

© COPYRIGHT UPM

Maeda, T., Meguro, S. and Takata, M. (1989). Isothermal capacitance transient spectroscopy in ZnO varistor. *Japanese Journal of Applied Physics. 28*(4): L714-L716.

Mandal, S. K., Das, A. K., Nath, T. K. and Karmakar, D. (2006). Temperature dependence of solubility limits of transition metals (Co, Mn, Fe, and Ni) in ZnO nanoparticles. *Applied Physics Letters. 89*(14): 144105-144105-144103.

Matsuoka, M. (1971). Nonohmic properties of zinc oxide ceramics. *Journal Applied Physics. 10*(6).

Matsuoka, M., Masuyama, T. and Lida, Y. (1969). Voltage nonlinearity of zinc oxide ceramics doped with alkali earth metal oxide. *Japanese Journal of Applied Physics. 8*(10): 1275-1276.

Mei, L.-T., Hsiang, H.-I., Hsi, C.-S. and Yen, F.-S. (2013). Na_2CO_3 doping effect on ZnO–Pr_6O_{11}–Co_3O_4 ceramic varistor properties. *Journal of Alloys and Compounds. 558*(0): 84-90.

Mielcarek, W., Nowak-woźny, D., Prociów, K. and Gubański, A. (2002). Thermally stimulated currents as a measure of degradation of zinc oxide varistors. *Radiation Effects and Defects in Solids. 157*(6-12): 1051-1055.

Milošević, O., Marinković, Z., Mančić, L. and Vulić, P. (2004). *The Influence of mechanical activation on the stoichiometry and defect structure of a sintered ZnO-Cr_2O_3 System.* Paper presented at the Materials Science Forum.

Mishra, U. and Singh, J. (2007). *Semiconductor device physics and design*. Dordrecht: Springer.

Modine, F. A. and Wheeler, R. B. (1990). Pulse response characteristics of ZnO varistors. *Journal Applied Physics. 67*(10): 6560-6066.

Mukae, K., Tsuda, K. and Nagasawa, I. (1977). Non-Ohmic properties of ZnO-rare earth metal oxide-Co_3O_4 ceramics. *Japanese Journal of Applied Physics. 16*(8): 1361-1368.

Mukae, K., Tsuda, K. and Nagasawa, I. (1979). Capacitance-vs-voltage characteristics of ZnO varistors. *Journal Applied Physics. 50*(6): 4475-4476.

© COPYRIGHT UPM

Nahm, C.-W. (2001). The electrical properties and d.c. degradation characteristics of Dy_2O_3 doped Pr_6O_{11}-based ZnO varistors. *Journal of the European Ceramic Society. 21*(4): 545-553.

Nahm, C.-W. (2003). Electrical properties and stability of praseodymium oxide-based ZnO varistor ceramics doped with Er_2O_3. *Journal of the European Ceramic Society. 23*(8): 1345-1353.

Nahm, C.-W. (2005). Effect of La_2O_3 addition on microstructure and electrical properties of ZnO-Pr_6O_{11}-based varistor ceramics. *Journal of Materials Science: Materials in Electronics. 16*(6): 345-349.

Nahm, C.-W. (2008a). Microstructure, electrical properties, and dc aging characteristics of Tb_4O_7-doped ZnO-based varistors. *Journal of Materials Science. 43*(8): 2857-2864.

Nahm, C.-W. (2009). The preparation of a ZnO varistor doped with and its properties. *Solid State Communications. 149*(19–20): 795-798.

Nahm, C.-W. (2011a). Effect of Mn doping on electrical properties and accelerated ageing behaviours of ternary ZVM varistors. *Bulletin Materials Science. 34*(7): 1385-1391.

Nahm, C.-W. (2011b). Pulse aging behavior of ZnO–Pr_6O_{11}–CoO–Cr_2O_3–Dy_2O_3 varistor ceramics with sintering time. *Ceramics International. 37*(4): 1409-1414.

Nahm, C.-W. (2012). Sintering effect on ageing behavior of rare earths (Pr_6O_{11}-Er_2O_3-Y_2O_3)-doped ZnO varistor ceramics. *Journal of Rare Earths. 30*(10): 1028-1033.

Nahm, C.-W. and Park, C.-H. (2000). Microstructure, electrical properties, and degradation behavior of praseodymium oxides-based zinc oxide varistors doped with Y_2O_3. *Journal of Materials Science. 35*(12): 3037-3042.

Nahm, C. W. (2008b). The effect of sintering temperature on varistor properties of (Pr, Co, Cr, Y, Al)-doped ZnO ceramics. *Materials Letters. 62*(29): 4440-4442.

Nitayama, A., Sakaki, H. and Ikoma, T. (1980). Properties of deep levels in ZnO varistors and their effect on current-response characteristics. *Japanese Journal of Applied Physics. 19*(12): L743-L746

© COPYRIGHT UPM

Ohashi, N., Mitarai, S., Fukunaga, O. and Tanaka, J. (1999). Magnetization and electric properties of Pr-doped ZnO. *Journal of Electroceramics. 4*(1): 61-68.

Ohbuchi, Y., Kawahara, T., Okamoto, Y. and Morimoto, J. (2001). Distributions of interface states and bulk traps in ZnO varistors. *Japanese Journal of Applied Physics. 40*(1): 213.

Ohbuchi, Y., Kawahara, T., Okamoto, Y. and Morimoto, J. (2002). Characterization of interface states in degraded ZnO Varistor. *Japanese Journal of Applied Physics. 41*: 190-196.

Olsson, E. and Dunlop, G. L. (1989). Characterization of individual interfacial barriers in a ZnO varistor material. *Journal of Applied Physics. 66*(8): 3666-3675.

Orlandi, M. O., Bomio, M. R. D., Longo, E. and Bueno, P. R. (2004). Nonohmic behavior of SnO_2-MnO polycrystalline ceramics. II. Analysis of admittance and dielectric spectroscopy. *Journal of Applied Physics. 96*(7): 3811-3817.

Ozgur, U., Alivov, Y. I., Liu, C., Teke, A., Reshchikov, M., Dogan, S., Avrutin, V., Cho, S.-J. and Morkoc, H. (2005). A comprehensive review of ZnO materials and devices. *Journal of Applied Physics. 98*(4): 0413011-041301103.

Palmisano, P., Biamino, S., Fino, P. and Badini, C. (2005, 3-6 April 2005). *Catalytic activity of rare earth perovskites towards soot combustion.* Paper presented at the European Combustion Meeting - ECM 2005, Louvain-la-Neuve, Belgium.

Pan, W. H., Kuo, S. T., Tuan, W. H. and Chen, H. R. (2010). Microstructure-property relationships for low voltage varistors. *International Journal of Applied Ceramic Techology. 7*(S1): E80-88.

Peng, Z., Fu, X., Zang, Y., Fu, Z., Wang, C., Qi, L. and Miao, H. (2010). Influence of Fe_2O_3 doping on microstructural and electrical properties of ZnO–Pr_6O_{11} based varistor ceramic materials. *Journal of Alloys and Compounds. 508*(2): 494-499.

Philipp, H. R. and Levinson, L. M. (1979). High temperature behaviour of ZnO based ceramic varistors. *Journal of Applied Physics. 50*(1): 383-389.

Pierret, R. F. (1996). *Semiconductor device fundamentals* Purdue University: Addison-Wesley Publishing Company.

© COPYRIGHT UPM

Pike, G. E. (1981). *Electronic Properties of ZnO Varistors: A New Model.* Paper presented at the MRS Proceedings.

Popa, M. and Kakihana, M. (2001). Synthesis and thermoanalytical investigation of an amorphous praseodymium citrate. *Journal of Thermal Analysis and Calorimetry. 65*(1): 281-293.

Prasad, B. V., Rao, G. N., Chen, J. and Babu, D. S. (2011). Relaxor ferroelectric like giant permittivity in $PrCrO_3$ semiconductor ceramics. *Materials Chemistry and Physics. 126*(3): 918-921.

Puyané, R., Toal, F. and Hampshire, S. (1996). Production of doped ZnO powders for varistor applications using sol-gel techniques. *Journal of Sol-gel Science and Technology. 6*(3): 219-225.

Ramírez, M. A., Bassi, W., Bueno, P. R., Longo, E. and Varela, J. A. (2008a). Comparative degradation of ZnO- and SnO_2 -based polycrystalline non-ohmic devices by current pulse stress. *Journal of Physics D: Applied Physics. 41*(12): 1220021-1220025.

Ramírez, M. A., Fernández, J. F., Frutos, J. d., Bueno, P. R., Longo, E. and Varela, J. A. (2010). Microstructural and nonohmic properties of $ZnO.Pr_6O_{11}.CoO$ polycrystalline system. *Materials Research. 13*: 29-34.

Ramírez, M. A., Rubio-Marcos, F., Fernández, J. F., Lengauer, M., Bueno, P. R., Longo, E. and Varela, J. A. (2008b). Mechanical properties and dimensional effects of ZnO- and SnO_2-based varistors. *Journal of the American Ceramic Society. 91*(9): 3105-3108.

Ramírez, M. A., Tararam, R., Simões, A. Z., Ries, A., Longo, E. and Varela, J. A. (2013). Degradation analysis of the SnO_2 and ZnO-based varistors using electrostatic force microscopy. *Journal of the American Ceramic Society. 96*(6): 1801-1809.

Rath, C., Singh, S., Mallick, P., Pandey, D., Lalla, N. P. and Mishra, N. C. (2009). Effect of cobalt substitution on microstructure and magnetic properties in ZnO nanoparticles. *Indian Journal of Physics. 83*(4): 415-421.

© COPYRIGHT UPM

Ribeiro, P. C., da Costa, E. G., Gama, L., Costa, A. C. F. d. M. and Kiminami, R. H. G. A. (2005). Chemical synthesis by Pechini method for obtation of ZnO varistors. *Materials Science Forum. 498 - 499*: 299-304.

Rohatgi, A., Pang, S. K., Gupta, T. K. and Straub, W. D. (1988). The deep level transient spectroscopy studies of a ZnO varistor as a function of annealing. *Journal of Applied Physics. 63*(11): 5375-5379.

Roy, P. K. (2012). Synthesis of nano ZnO powder and study of its varistor behavior at different temperatures. *Journal of Materials Science Research. 1*(4): 28-34.

Sabri, M. G. M., Azmi, B. Z., Zahid, R., Halimah, M. K., Hashim, M. and Sidek, H. A. A. (2009). Application of direct current and temperature stresses of low-voltage ZnO based varistor ceramics. *American Journal of Applied Science. 6*(8): 1591-1595.

Santos, M. R. C., Bueno, P. R., Longo, E. and Varela, J. A. (2001). Effect of oxidizing and reducing atmospheres on the electrical properties of dense SnO_2-based varistors. *Journal of the European Ceramic Society. 21*(2): 161-167.

Sato, K., Takada, Y., Maekawa, H., Ototake, M. and Tominaga, S. (1980). Electrical Conduction of ZnO Varistors under Continuous DC Stress. *Japanese Journal of Applied Physics. 19*(5): 909-917.

Sato, Y., Mizoguchi, T., Oba, F., Yodogawa, M., Yamamoto, T. and Ikuhara, Y. (2004a). Identification of native defects around grain boundary in Pr-doped ZnO bicrystal using electron energy loss spectroscopy and first-principles calculations. *Applied Physics Letters 84*(26): 5311-5313.

Sato, Y., Oba, F., Yodogawa, M., Yamamoto, T. and Ikuhara, Y. (2004b). Grain boundary dependency of nonlinear current–voltage characteristics in Pr and Co Doped ZnO Bicrystals. *Journal Applied Physics. 95*(3): 1258-1264.

SemiLab. (2003). DLS-83 user manual. Budapest, Hungary: Semiconductor Laboratory Inc.

Senda, T. and Bradt, R. C. (1990). Grain growth in sintered ZnO and ZnO-Bi_2O_3 ceramics. *Journal of the American Ceramic Society. 73*(1): 106-114.

© COPYRIGHT UPM

Si, P. Z., Wang, H. X., Jiang, W., Lee, J. G., Choi, C. J. and Liu, J. J. (2011). Synthesis, structure and exchange bias in $Cr_2O_3/CrO_2/Cr_2O_5$ particles. *Thin Solid Films. 519*(23): 8423-8425.

Simpson, J. C. and Cordaro, J. F. (1988). Characterization of deep levels in zinc oxide. *Journal Applied Physics. 63*(5): 1781-1783.

Simpson, J. C. and Cordaro, J. F. (1990). Defect clusters in zinc oxide. *Journal of Applied Physics. 67*(11): 6760-6763.

Singh, S., Senthil Kumar, E. and Ramachandra Rao, M. S. (2008). Microstructural, optical and electrical properties of Cr-doped ZnO. *Scripta Materialia. 58*(10): 866-869.

Solorzano, I. G., Sande, J. B. V., Baek, K. K. and Tuller, H. L. (1992). Compositional analysis and high resolution imaging of grain boundaries in Pr-doped ZnO ceramics. *MRS Online Proceedings Library. 295*.

Sonder, E., Austin, M. M. and Kinser, D. L. (1985). Effect of oxidizing and reducing atmospheres at elevated temperature on the electrical properties of zinc oxide varistor. *Journal of Applied Physics. 54*(6): 3566-3572.

Souza, F. L., Gomes, J. W., Bueno, P. R., Cassia-Santos, M. R., Araujo, A. L., Leite, E. R., Longo, E. and Varela, J. A. (2003). Effect of the addition of ZnO seeds on the electrical proprieties of ZnO-based varistors. *Materials Chemistry and Physics. 80*(2): 512-516.

Stucki, F. and Greuter, F. (1990). Key role of oxygen at zinc oxide varistor grain boundaries. *Applied Physics Letters. 57*(5): 446-448.

Sun, Y.-f., Liu, S.-B., Meng, F.-l., Liu, J.-Y., Jin, Z., Kong, L.-T. and Liu, J.-H. (2012). Metal oxide nanostructures and their gas sensing properties: A review. *Sensors. 12*: 2610-2631.

Suzuki, H. and Bradt, R. C. (1995). Grain Growth of ZnO in $ZnO\text{-}Bi_2O_3$ Ceramics with TiO_2 Additions. *Journal of the American Ceramic Society. 78*(5): 1354-1360.

Tada, T. (2010). Degradation of ZnO varistors as estimated by aging tests. *Electrical Engineering in Japan. 170*(2): 1-18.

© COPYRIGHT UPM

Takehana, M., Nishino, T., Sugawara, K. and Sugawara, T. (1996). Preparation of zinc oxide varistor by a wet chemical method. *Materials Science and Engineering: B. 41*(1): 186-189.

Tanaka, A. and Mukae, K. (1999). ICTS measurements of single grain boundaries in ZnO: Rare-earth varistor. *Journal of Electroceramics. 4*(1): 55-59.

Tao, M., Ai, B., Dorlanne, O. and Loubiere, A. (1987). Different "single grain junctions" within a ZnO varistor. *Journal of Applied Physics. 61*(4): 1562-1567.

Toplan, H. O. and Karakas, Y. (2002). Grain growth in TiO_2-added ZnO-Bi_2O_3-CoO-MnO ceramics prepared by chemical processing. *Ceramic International. 28*: 911-915.

Varela, J. A., Cerri, J. A., Leite, E. R., Longo, E., Shamsuzzoha, M. and Bradt, R. C. (1999). Microstructural evolution during sintering of CoO doped SnO_2 ceramics. *Ceramics International. 25*(3): 253-256.

Vines, L., Wong-Leung, J., Jagadish, C., Quemener, V., Monakhov, E. V. and Svensson, B. G. (2012). Acceptor-like deep level defects in ion-implanted ZnO. *Applied Physics Letters. 100*(21): 212106-212106-212104.

Vipin, P. M., Sanjaynath, V. V., Varma, H. K., Warrier, K. G. K. and Damodaran, A. D. (1989). Non-linearity in rare earth doped zinc oxide varistor prepared by flash combustion method. *Journal of the European Ceramic Society. 5*(4): 233-236.

Wakiya, N., Chun, S.-Y., Lee, C. H., Sakurai, O., Shinozaki, K. and Mizutani, N. (1999). Effect of liquid phase and vaporization on the formation of microstructure of Pr doped ZnO varistor. *Journal of Electroceramics. 4*(0): 15-23.

Wang, M.-H., Hu, K.-A., Zhao, B.-Y. and Zhang, N.-F. (2007a). Degradation phenomena due to humidity in low voltage ZnO varistors. *Ceramics International. 33*(2): 151-154.

Wang, M.-H., Yao, C. and Zhang, N.-F. (2008). Degradation characteristics of low-voltage ZnO varistor manufactured by chemical coprecipitation processing. *Journal of Materials Processing Technology. 202*(1–3): 406-411.

© COPYRIGHT UPM

Wang, Y.-P., Lee, W.-I. and Tseng, T.-Y. (1996). Degradation phenomena of multilayer ZnO-glass varistors studied by deep level transient spectroscopy. *Applied Physics Letters. 69*(12): 1807-1809.

Wang, Y., Li, S., Zhang, M., Cheng, P., Lin, Y. and Alim, M. (2007b). Improvement of energy-handling capability of the ZnO varistors prepared by fractional precipitation on the seed materials. *Journal of Materials Science: Materials in Electronics. 18*(5): 495-503.

Wei, K., Guo, W., Du, C., Zhao, N. and Li, X. (2009). Preparation of $Pr_xZn_{1-x}O$ nanopowder with UV-visible light response. *Materials Letters. 63*(21): 1781-1784.

Westin, G., Ekstrand, A., Nygren, M., Osterlund, R. and Merkelbach, P. (1994). Preparation of ZnO-based varistors by the sol-gel technique. *Journal of Materials Chemistry. 4*(4): 615-621.

Winston, R. A. and Cordaro, J. F. (1990). Grain-boundary interface electron traps in commercial zinc oxide varistors. *Journal Applied Physics. 68*(12): 6495-6500.

Wurst, J. C. and Nelson, J. A. (1972). Lineal intercept technique for measuring grain size in two-phase polycrystalline ceramics. *Journal of the American Ceramic Society. 55*(2): 109-109.

Yang, W., Zhou, D., Yin, G., Wang, R. and Zhang, Y. (2005). Characterization of ZnO based varistor derived from nano ZnO powders and ultrafine dopants. *Journal of Materials Science and Technology. 21*(2): 183-186.

Yano, Y., Shirakawa, Y. and Morooka, H. (1992). Deep-level transient spectroscopy of interface states in $ZnO/PrCoO_x/ZnO$ thin-film junctions. *Japanese Journal of Applied Physics. 31*: L1429-L1431.

Yongvanich, N., Visuttipitukkul, P., Parnem, R., Sittikeadsakun, A. and Wittayaprasopchai, A. (2011). Influence of chromium on microstructure and electrical properties of ZnO-based varistor materials. *Energy Procedia. 9*: 474-482.

Yoshida, H., Takada, M. and Yoshikado, S. (2008). Study on the recovery of electrical degradation of ZnO varistors. *Key Engineering Materials. 350*: 209-212.

© COPYRIGHT UPM

Zhang, L. (2004). Preparation of multicomponent ceramic nanoparticles. Group Inorganic Material Literature Review. 1-29. Retrieved from http://www.matsceng.ohio-state.edu/ims/LR_Multioxides.pdf

Zhang, M., Liu, F. and Liu, Z. (1991). Studies on degradation mechanism of ZnO varistor under impulse stress by thermally stimulated current Vol. 1. *Proceedings of the 3rd International Conference on Properties and Applications of Dielectric Materials, 1991* (pp. 513-516).

Zhou, D., Zhang, C. and Gong, S. (2003). Degradation phenomena due to dc bias in low-voltage ZnO varistors. *Materials Science and Engineering: B. 99*(1–3): 412-415.

Zhu, J. F., Gao, J. Q., Wang, F. and Chen, P. (2008). Influence of Pr_6O_{11} on the characteristics and microstructure of zinc varistors. *Key Engineering Materials. 368 - 372*: 500-502.

© COPYRIGHT UPM